THESIS

CHARACTERIZATION OF SOLIDS IN PRODUCED WATER FROM WELLS

FRACTURED WITH RECYCLED AND FRESH WATER

Submitted by

Gen Li

Department of Civil and Environmental Engineering

In partial fulfillment of the requirements

For the Degree of Master of Science

Colorado State University

Fort Collins, Colorado

Summer 2015

Master's Committee:

    Advisor: Kenneth H. Carlson

    Pinar Omur-Ozbek
    Thomas H. Bradley

ABSTRACT

CHARACTERIZATION OF SOLIDS IN PRODUCED WATER FROM WELLS FRACTURED WITH RECYCLED AND FRESH WATER

Water management is a central issue in oil and gas development. Hydraulic fracturing applied in unconventional tight oil and gas development requires large amounts of water, and the wastewater that results after production--containing high levels of organic and inorganic matter--usually is disposed of through deep well injection. A new approach reuses this produced water as part of subsequent fracturing fluid, an alternative that could significantly reduce both fresh water demand and the cost associated with deep well injection. However, produced water must be treated prior to reuse, to remove most of the suspended solids and multivalent ions that would otherwise cause scale or clogging problems. Understanding the amount and composition of solids in produced water is crucial in achieving optimized treatment and reuse.

This study targeted the characterization, both qualitatively and quantitatively, of the solids in produced water from oil and gas operations and the comparison of solids from wells fractured with fresh water and recycled water. Samples were collected from five wells at the Crow Creek and Chandler State pads in the Wattenberg field of Northern Colorado. Wells in the same pad were fractured either with fresh surface water only or with water blended with some portion of recycled produced water. Gravimetric analyses of dissolved and suspended solids were performed, and particle size distributions of suspended solids were measured. Suspended solids also were isolated and characterized with X-ray photoelectron spectroscopy (XPS).

Gravimetric analyses showed that total dissolved solids (TDS) averaged about 24000 mg/L and 17000 mg/L for Crow Creek and Chandler State wells, respectively. Total suspended

solids (TSS) concentrations were much lower, measuring 550 and 260 mg/L for the two pads. About 9 to25 percent of TDS was volatile and 88 to 99 percent of TSS was highly volatile. Particle sizes were high during first few days of production and then stabilized at about 400 nm and 900 nm for wells on the Crow Creek and Chandler State pads, respectively. At the Crow Creek pad, particle sizes were smaller and mono-distributed in produced water samples collected during the first week of production from the well fractured with recycled water, suggesting that the recycled water was more compatible with shale formation and that wells fractured with recycled water tend to clean out faster. XPS tests for isolated suspended solids showed the presence of major elements such as oxygen, carbon, and silicon, along with minor elements such as calcium, magnesium, zirconium, iron, and others. Core-level scanning confirmed that the isolated suspended solids were mainly composed of carbonate based minerals and metal oxides; several iron compounds with different valences were also found in the produced water samples.

TABLE OF CONTENTS

LIST OF TABLES

LIST OF FIGURES

1 Introduction

As hydraulic fracturing and horizontal drilling technologies are increasingly applied to unlock the tremendous potential in tight shale plays, a significant amount of water is used in the drilling and, in particular, the fracturing process. The produced water generated during hydraulic fracturing and then separated from the oil and gas products is becoming the largest waste stream in the industry: about 30 percent of this fracturing fluid flows back as wastewater in the first month of production. Instead of disposing this wastewater through deep well injection, oil and gas producers are making the effort to reuse produced water as the base for new fracturing fluid. The make-up of this produced water can be complex and can include emulsified oil and grease, suspended and dissolved solids, heavy metals, and chemical additives from fracturing fluid mixtures formulated to enhance oil and gas recovery. Produced water composition also can vary significantly between different geographic locations and formation properties. Knowing the quality of produced water provides more insight for potential beneficial reuse and helps optimize the treatment necessary for such reuse.

In this study, a comprehensive characterization of the suspended solids in produced water was completed. Produced water samples were collected from five wells at the Crow Creek and Chandler State pads in the Wattenberg Field of Northern Colorado. Gravimetric analyses identified the total dissolved solids (TDS), total suspended solids (TSS), and the volatile potion of each solids category. Particle sizes and distribution were measured using a dynamic light scattering method and results analyzed. Suspended solids were successfully isolated and characterized with X-ray photoelectron spectroscopy.

Chapter 2 of this paper provides an overview of technology advances in unconventional oil and gas development. Previous work on produced water characterization is discussed, and gaps in the knowledge of this subject matter are identified.

Chapter 3 provides additional information on sampling methods and experimental procedures. The underlying principles of particle sizing and X-ray photoelectron spectroscopy (XPS) are also discussed. Full method descriptions are also available in the method section of chapter 4.

Chapter 4 includes a journal paper prepared for submission to the journal of Energy & Fuel. The article was reformatted to fit the thesis-formatting requirements. This paper includes a brief introduction section, full method descriptions, and a summary of results and discussions section.

Raw data on particle sizing and XPS spectra are included in Appendix A and Appendix B, respectively.

2   Literature Review

2.1   Unconventional Oil and Gas Development

Oil and gas are the main sources of energy worldwide. The U.S. Energy Information

Administration (EIA, 2014) estimated that 65 percent of energy consumption in the U.S. comes

from oil and natural gas sources and projected that domestic demand for fossil fuel will remain

high through 2040. By accommodating its growing energy demand, the U.S. saw in 2009 its first

growth in annual oil production since 1991; and since 2012, the country has led the world in

petroleum and natural gas production (Doman, 2015) (Table 2-1).

Table 2-1. 2000-2014 U.S annual oil and gas production

Year	Crude oil production (MMbbl/d)	Dry natural gas production (tcf)
2000	5.822	19.182
2001	5.801	19.616
2002	5.744	18.928
2003	5.649	19.099
2004	5.441	18.591
2005	5.181	18.051
2006	5.088	18.504
2007	5.077	19.266
2008	5.000	20.159
2009	5.350	20.624
2010	5.482	21.315
2011	5.645	22.901
2012	6.497	24.033
2013	7.461	24.333
2014	8.663	25.718

Data source: EIA, 2015a; EIA, 2015b

The main U.S. oil growth margin is identified as coming from tight shale formation

development. Tight oil production has increased dramatically from less than 1 million barrels

per day (MMbbl/d) in 2010 to more than 3 MMbbl/d in 2013 (EIA, 2014). Further, BP Energy

(2014) projected that U.S. tight oil output will increase by about 3 MMbbl/d to more than

5MMbbl/d in 2035.

In 2013, U.S. crude oil and lease condensate proved reserves increased to 36.5 billion

barrels, reflecting a five-year increase and a 9.3 percent increase from the 2012 estimate. The

Bakken/Three Forks play and Eagle Ford play (Figure 2-1) are the largest tight oil plays in the

United States, with proved reserves of 4844 and 4177 million barrels of crude oil, as of 2013,

respectively. The study detailed in this report focused on the area of the Denver-Julesburg basin

(Niobrara formation), located in Northern Colorado.
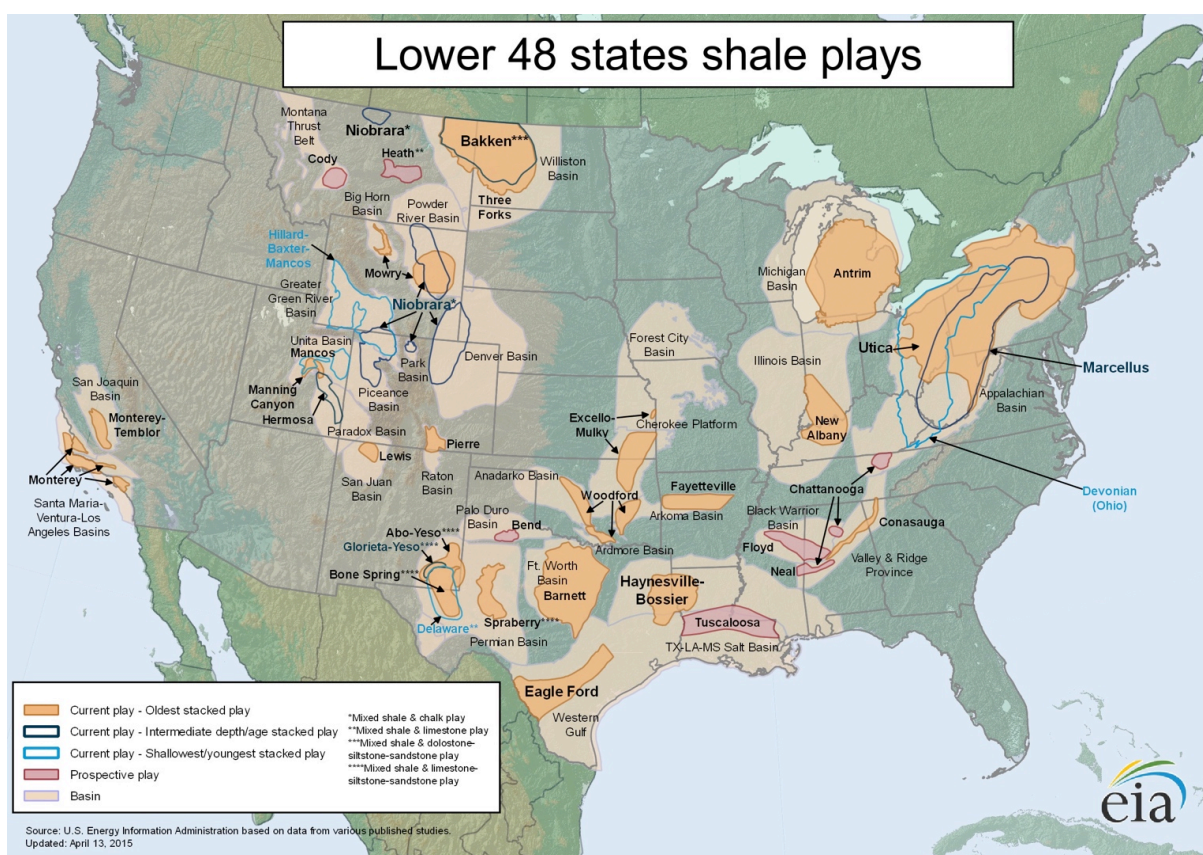
Figure 2-1. Map of U.S. shale gas and shale oil plays (EIA, 2015c)

2.2   Hydraulic Fracturing and Horizontal Drilling

A hydrocarbon-bearing formation with dispersed oil and gas content is considered "unconventional" (Lechtenböhmer et al., 2011). The oil content per rock volume ratio in these formations is so small that a conventional vertical well will have only limited access to the reservoir, and it will not produce an economic flow. Another distinct characteristic is the low permeability of the shale formation. Shale rock is a clay-rich, fine-grained sedimentary source rock that contains matured hydrocarbon and natural gas. The permeability of a shale tight formation is usually in the range of 0.1- 0.0001 millidarcies (md) (Figure 2-2).
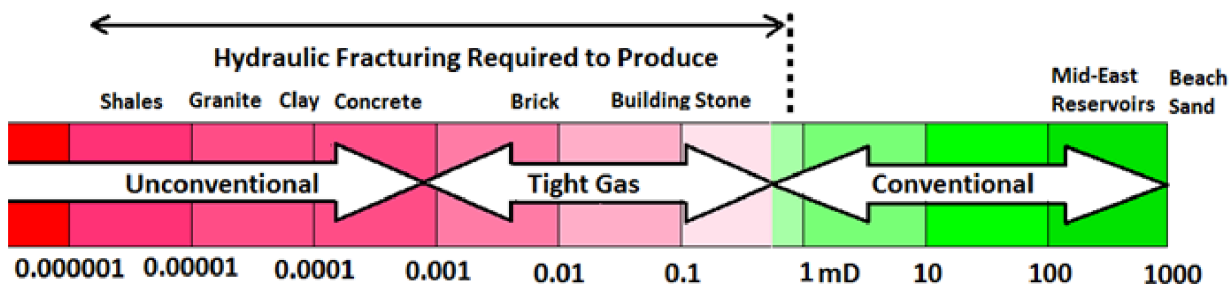
Figure 2-2. Permeability range of producing formations, showing where fracturing is required (King, G. E., 2012)

Horizontal drilling technology has expanded reservoir access, and hydraulic fracturing is now employed to open up small fractures through the tight shale formation. Wells are drilled vertically to the target depth (usually 2000-6500 ft) and then gradually turned to a horizontal direction within oil-bearing strata. Wells can extend up to one mile horizontally (Figure 2-3).

Horizontal drilling also has changed well siting and construction management practices. Locations of vertical wells often are scattered over the field and constructed separately. However, wells drilled horizontally can be arranged in a condensed area and constructed all at once--an approach that will significantly reduce production, waste management, and

transportation costs as well as environmental impact by reducing surface area footprint and disturbance.
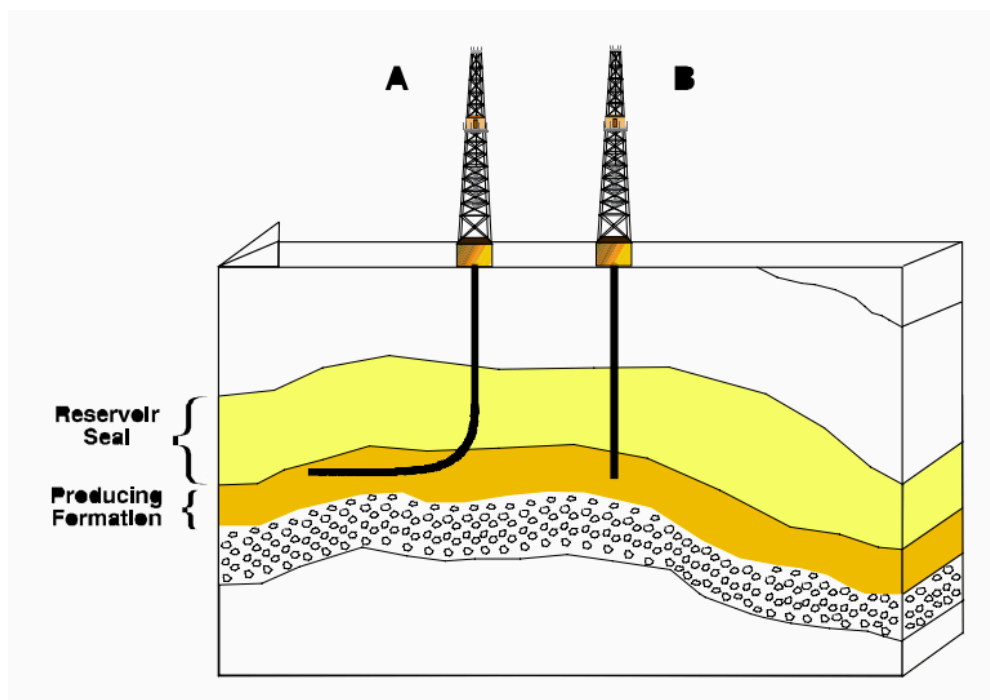
Figure 2-3. Wellbore of horizontal well A sees more exposure to producing formation than that of vertical well B (King and Morehouse, 1993)

High-pressure fracturing fluid, composed of freshwater (90%), sand (9.5%), and chemical additives (0.5%), is injected into the wellbore to create and maintain fissure systems that allow trapped hydrocarbons to flow throughout. Table 2-2 lists some of the chemical additives and their intended purposes. Ingredients such as sand and cross-linked gel could contribute to suspended solids as they flow back to surface. Also, surfactant creates oil-in-water emulsions, requiring demulsifier to promote coalescence during the produced water treatment process.

Table 2-2. Chemical additives in shale gas extraction (Bishop, n.d)

Additive Type	Examples	Purpose	Used In
Friction Reducer	heavy naphtha, polymer microemulsion	lubricate drill head, penetrate fissures	drilling muds, fracturing fluids
Biocide	glutaraldehyde, DBNPA, dibromoacetonitrile	prevent biofilm formation	drilling muds, fracturing fluids
Scale Inhibitor	ethylene glycol, EDTA, citric acid	prevent scale buildup	drilling muds, fracturing fluids
Corrosion Inhibitor	propargyl alcohol, N,N-dimethylformamide	prevent corrosion of metal parts	drilling muds, fracturing fluids
Clay Stabilizer	tetramethylammonium chloride	prevent clay swelling	drilling muds, fracturing fluids
Gelling Agent	bentonite, guar gum, "gemini quat" amine	prevent slumping of solids	drilling muds, fracturing fluids
Conditioner	ammonium chloride, potassium carbonate, isopropyl alcohol	adjust pH, adjust additive solubility	drilling muds, fracturing fluids
Surfactant	2-butoxyethanol, ethoxylated octylphenol	promote fracture penetration	drilling fluids, fracturing fluids
Cross-Linker	sodium perborate, acetic anhydride	promote gelling	fracturing fluids
Breaker	hemicellulase, ammonium persulfate, quebracho	"breaks" gel to promote flow-back of fluid	post-fracturing fluids
Cleaner	hydrochloric acid	dissolve debris	stimulation fluid, pre-fracture fluid
Processor	ethylene glycol, propylene glycol	strip impurities from produced gas	post-production processing fluids

2.3   Economic and Environmental Impacts

2.3.1 Economic Impact

After the financial crisis in 2007 that caused weak economic growth and a high unemployment rate, the shale gas revolution provided a strong boost for the U.S. economy. The booming shale gas production has brought adequate supply and low energy prices to production and manufacturing industries, stimulating the U.S. economic recovery in the manufacturing

sector. The production growth of crude oil and natural gas also gradually reduced foreign oil imports, which strengthened U.S. energy independence.

According to a report from IHS Global Insight (2011), the main economic benefits of the U.S. shale gas revolution are as follows:

- The first benefit is the promotion of economic growth and an increase in the employment rate. In 2010 alone, shale gas-related industries realized a $760 billion GDP and more than 600,000 new jobs; this growth is expected to continue in the future.

- The second benefit is the creation of additional tax revenue. Shale gas-related industries contributed $18.6 billion of tax at local, state, and federal government levels in the year of 2010.

- Thirdly, unconventional shale development can reduce energy costs and enhance the competitiveness of related industries. In 2011, drilling costs of unconventional gas wells saw a 40 to 50 percent reduction, compared to conventional natural gas wells. In the mean time, lower natural gas prices decreased electricity prices for industries by 10 percent and allowed a 2.9 percent increase in industrial production.

2.3.2 Environmental impacts

The growth of unconventional drilling activities throughout major basins in the U.S. has raised public concerns regarding environmental and public health related issues. Proper risk management and the application of best engineering practices are expected to help mitigate these threads. Environmental impacts of shale oil and gas development could include:

(1) Water pollution. The large water demand of shale gas extraction could intensify competition of water resources, especially in water-scarce areas. A report from the International

Energy Agency (IEA) noted that harmful substances could penetrate or spill into the underground aquifer and contaminate sources of drinking water; natural gas also could dissolve into an adjacent reservoir (Birol et al., 2011). However, a report released by MIT (2011) showed that, over the past ten years, in over 20,000 or more shale gas wells nationwide, only 43 water pollution incidents were reported--an indication that ground water contamination can be controlled and the risk of such can be minimized.

(2) Air pollution and greenhouse gas emissions. Natural gas can be considered a transition from coal-based energy to a future, renewable energy form. Natural gas is much cleaner than coal, typically emitting low sulfur dioxide, carbon monoxide and fine particles (PM 2.5 and PM 10). Notwithstanding, natural gas does contribute to global greenhouse emissions; with the greenhouse effect of methane being 25 times larger than CO2, a possible natural gas leak through gas extraction and transportation can contribute significantly to the greenhouse effect (Riemer, 1996).

(3) Small earthquakes. Hydraulic fracturing and deep-well injection can increase the possibility of small earthquakes. Although a strong cause-effect relationship has not been established, the increase of small earthquakes with active hydraulic fracturing activities has been recorded since the 1980s (Fehler et al., 1987;Sasaki, 1998). The U.S. Department of Geological Survey (USGS) has noted that the number of recorded earthquakes with $M \geq 3$ was five times greater in 2011 and 2012, compared to the yearly rate from 2000 to 2010 and that most were injection-induced earthquakes (Ellsworth, 2013).

2.4 Water Management

2.4.1 Water Demand

The water demand of well development primarily consists of two parts: drilling/well completion and reservoir stimulation (hydraulic fracturing). The water usage rate can vary significantly, for both drilling/well completion and reservoir stimulation, depending on the well type. Water-based drilling mud, consisting primarily of clay and chemical additives, is used to cool drill bits and carry rock cuttings to the surface. Vertical and directional wells are shorter than horizontal wells; thus, they use less water in drilling than a typical horizontal well, which requires a maximum of 600,000 gallons of water for drilling (COGA, 2015).

For hydraulic fracturing, a vertical well uses 100,000 to 1,000,000 gallons of water, if a stimulation step is included; in comparison, whereas a horizontal well uses 2 to 5 million gallons, depending on the length and the number of fracture stages. Table 2-2 summarizes average water usage per well for drilling and fracturing process and provides a rough estimate of total water demand. In the Wattenberg field, water use was estimated between 2.8 and 6.5 million gallons per well, respectively, for horizontal wells and extended horizontal wells that have fracture stages greater than 25 (Goodwin et al. 2013).

Table 2-3. Average water usage and water demand for major shale plays (Acharya et al., 2011)

	Average water usage (bbls/well)			Wells/year	Water demand MMbbls/year
	Drilling	Fracturing	Total		
Barnett	10,000	70,000	80,000	600	48
Fayetteville	1,500	70,000	71,500	250	18
Haynesville	25,000	65,000	90,000	200	18
Marcellus	2,000	90,000	92,000	600	55

2.4.2 Wastewater Production

The water that separates from hydrocarbon products at the surface is referred to as "flowback" or "produced water." In the early stage of well production, waste water flowing back consists primarily of fracturing fluid, broken cross linkers, chemical additives, clays, dissolved metal ions, and high levels of TDS and TSS. This "flowback" water has a high flow rate, and its water quality changes rapidly on a daily basis. As the well cleans itself up and the injected fracturing fluid reaches equilibrium with the formation, wastewater primarily contains dissolved organic matters and high levels of TSS and TDS, with elevated concentrations of magnesium, calcium, barium, and iron. Produced water flows throughout the extent of production, and flow rate gradually decreases until stabilized (Figure 2-4). However, the transition between flowback and produced water is not well defined. Generally, the flowback period takes a few days to several weeks.
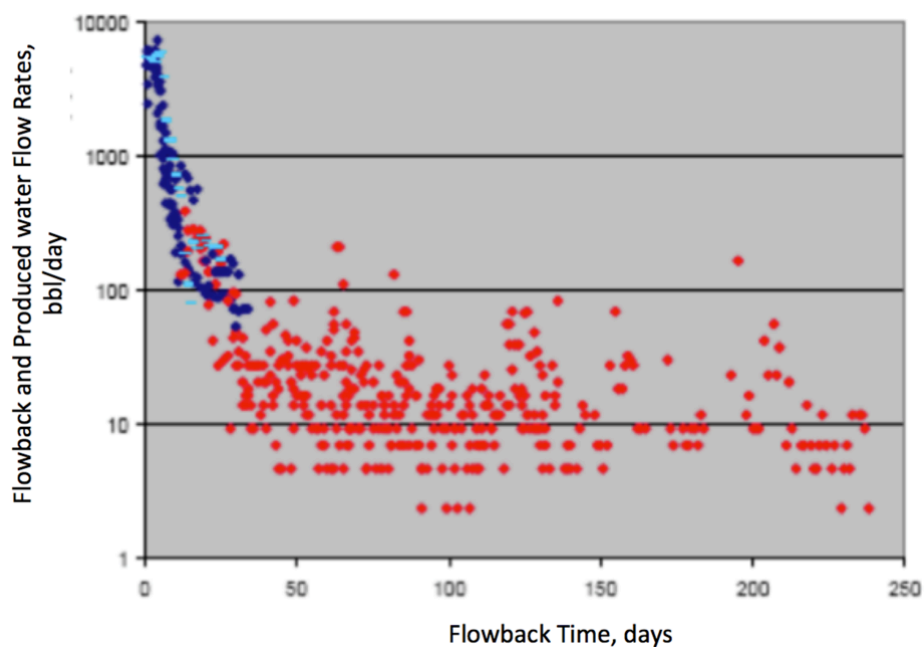

Figure 2-4. Flowback and produced water flow rates in the Marcellus shale. Blue points refer to "Flowback" and the red points refer to "Produced water." (Acharya et al., 2011)

11

The estimated amount of produced water generated in the United States is between 6.1×10^6 m³/day and 7.8×10^6 m³/day (1,600 and 2,060 million gallons/day) (Benko, 2008). Table 2-4 showed produced water generation for major geologic basins and the treatability potentials were categorized based on TDS concentrations.

Table 2-4. Produced water generation for major geologic basins (Benko, 2008)

Geologic basin	Water production m³/day	mg · day[a]	Median TDS (mg/L)[b]	Potential for treatment
Williston	18,000	4.9	132,400	Low
Powder River	370,000	97	7,300	Very high
Big Horn	360,000	94	4,900	Very high
Wind River	54,000	14	5,300	Very high
Green River	41,000	11	9,400	High
Denver	14,000	3.8	10,200	High
Uinta-Piceance	42,000	11	13,200	High
Paradox	21,000	5.6	67,000	Low
San Juan	14,000	3.6	22,700	Medium
Anadarko	34,000	8.9	132,200	Very low
Permian[c]	250,000	65	89,200	Low
San Joaquin	NA	NA	22,700	Medium
Los Angeles	NA	NA	30,330	Medium

[a]Boysan et al, 2002; [b]Breit and Otton, 2002; [c]for natural gas only and for the New Mexico portion of the Permian Basin.

A study (Ziemkiewicz, 2014) reported that, in the Marcellus field, about 10 to 30 percent of injected fracturing fluid returns to the surface and about 80 percent of that returned fluid is recycled as makeup water in subsequent fracturing activities. The remaining 20 percent of produced water is generally disposed of through deep-well injection (Figure 2-5).
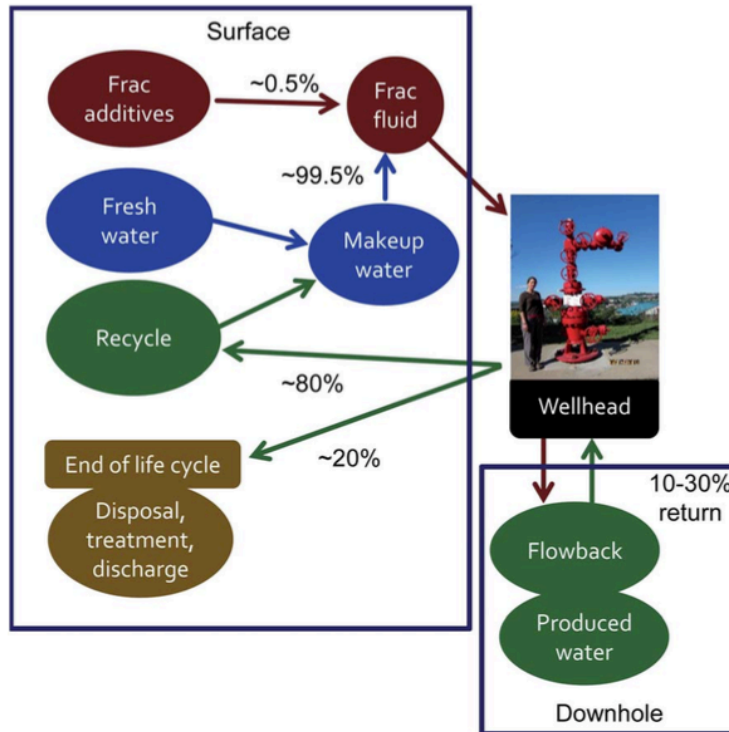
Figure 2-5. Water management components of a typical shale gas well (Ziemkiewicz, 2014)

2.5   Characteristics of Produced Water

Because produced water comes in contact with underground formation/brine water and dissolved minerals, it presents a complicated and highly variable water quality. The components of produced water can be categorized as inorganic salts, organic constituents, production solids, and naturally occurring radioactive material (NORM).

2.5.1 Inorganic salts

Inorganic constituents originate primarily from dissolved formation minerals. While the dominant salt in most produced water is sodium chloride, other cations such as K^+, Ca^{2+}, Mg^{2+}, Sr^{2+}, Ba^{2+}, Fe^{3+} and anions such as Cl^-, SO_4^{2-}, CO_3^{2-} and HCO_3^- can be present. Total dissolved solids (TDS) concentration in produced water ranges from 1,000 mg/L to more than 400,000 mg/L (Benko and Drewes, 2008). Sulfate concentration in produced water is usually lower than

that of seawater. An inorganic water quality summary from the Marcellus shale is provided in Table 2-5.

Table 2-5. Summary of Marcellus Shale Produced Water Quality (Barbot et al., 2013)

	minimum	maximum	average	number of samples
TDS (mg/L)	680	345,000	106,390	129
TSS (mg/L)	4	7,600	352	156
oil and grease (mg/L)	4.6	802	74	62
COD (mg/L)	195	36,600	15,358	89
TOC (mg/L)	1.2	1530	160	55
pH	5.1	8.42	6.56	156
alkalinity (mg/L as $CaCO_3$)	7.5	577	165	144
SO_4 (mg/L)	0	763	71	113
Cl (mg/L)	64.2	196,000	57,447	154
Br (mg/L)	0.2	1,990	511	95
Na (mg/L)	69.2	117,000	24,123	157
Ca (mg/L)	37.8	41,000	7,220	159
Mg (mg/L)	17.3	2,550	632	157
Ba (mg/L)	0.24	13,800	2,224	159
Sr (mg/L)	0.59	8,460	1,695	151
Fe dissolved (mg/L)	0.1	222	40.8	134
Fe total (mg/L)	2.6	321	76	141
gross alpha[a] (pCi/L)	37.7	9,551	1,509	32
gross beta[a] (pCi/L)	75.2	597,600	43,415	32
Ra^{228} (pCi/L)	0	1,360	120	46
Ra^{226} (pCi/L)	2.75	9,280	623	46
U^{235} (pCi/L)	0	20	1	14
U^{238} (pCi/L)	0	497	42	14

[a]Data for Northeast Pennsylvania only.

2.5.2 Organic Constituents

Produced water typically has a total organic carbon (TOC) concentration ranging from non-detectable to 1700 mg/L (Table 2-6), with pH and temperature the significant factors affecting the concentration of soluble organics. Organic constituents generally fall into two categories: dissolved and dispersed. Dissolved organics are often found in low- and medium-carbon ranges; formic acid and propionic acid are two typical compounds found in produced

water (Fakhru'l-Razi, 2009). Benzene, toluene, ethylbenzene, and xylene (BTEX) compounds

are the most common dissolved organic contents in produced water.

Table 2-6. Organic Material in Produced Water from Oil Operations (Guerra et al., 2011)

Constituent	Units	Concentration Range			Technique (Method)
		Low	High	Median	
TOC	mg/L	ND	1,700	NA	UV Oxidation/IR (USEPA 415.1)
COD	mg/L	1,220		NA	Redox Titration (USEPA 410.3)
TSS	mg/L	1.2	1,000	NA	Gravimetric (USEPA 160.2)
Total Oil	mg/L	2	565	NA	Gravimetric (USEPA 413.1)
Volatiles	mg/L	0.39	35	NA	GC/MS (USEPA 1624 Rev B and USEPA 24 & CLP)
Total Polars	mg/L	9.7	600	NA	Florisil column/IR
Phenols	mg/L	0.009	23	NA	Silylation GLC/MS
Volatile Fatty Acids	mg/L	2	4,900	NA	Direct GLC/FID of water

[1] ND = below detection limit; NA = not available.

Dispersed organic contents present as small droplets suspended in the produced water.

Less-soluble polyaromatic hydrocarbons (PAHs) and heavy phenols are usually found in

produced water as dispersed oil (Igunnu & Chen, 2012). "The amount of dispersed oil in

produced water depends on the density of oil, the shear history of the droplet, the amount of oil

precipitation, and interfacial tension between the water and oil." (Fakhru'l-Razi, 2009)

2.5.3 Naturally Occurring Radioactive Material (NORM)

Oil-field formation water that is rich in chloride enhances the solubility of radioactive

elements such as radium (Zielinski & Otton, 1999); this radium-bearing water is extracted to the

surface with oil and gas development. Radium will co-precipitate with barite (barium sulfate)

and deposit on oil field equipment. As shown in Table 2-5, [226]Radium and [228]Radium are the most abundant NORMs in produced water.

2.5.4 Production solids

A wide range of materials, including formation solids, corrosion and scale products, bacteria, waxes, and asphaltenes, make up the production solids in produced water (Fakhru'l-Razi, 2009).

Suspended particulates in a dispersed aqueous system, and the effects of settling time, mass transportation, aggregation pattern and colloidal chemical reaction, have been fully studied within the context of municipal wastewater research and management.   Four different size categories are usually applied to describe the pollution fractions in urban wastewater: soluble (<0.001 μm); colloidal (0.001–1 μm); supracolloidal (1–100 μm); and settleable (>100 μm) (Levine et. al.,1991). Total Suspended Solids (TSS) are those solids in supracolloid and settleable size ranges. Figure 2-4 identifies the size range of major organic compounds in municipal wastewater.
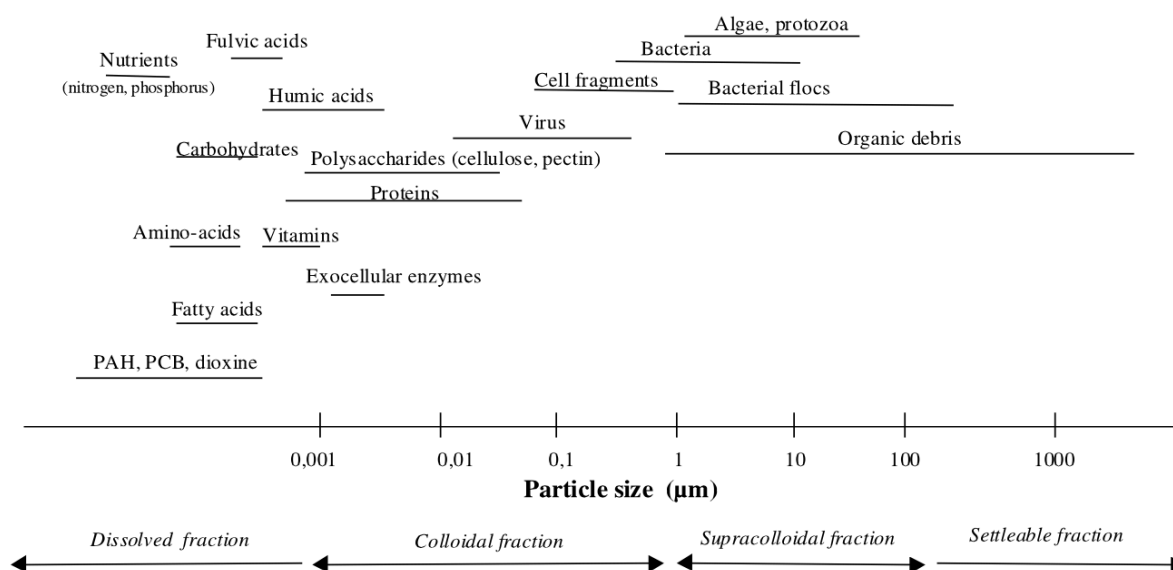

Figure 2-6. Size distribution of Contaminants in Urban Wastewater (Azema et al., 2002)

16

Azema et al. compared different optical methods for characterizing wastewater suspended solids and proposed laser granulometry method for a better discrimination of supracolloids and settleable particles. A more extensive review of methods such as light scattering, differential mobility analysis, time of flight mass spectroscopy (TOF-MS), microscopy, and surface area measurements showed that the dynamic light scattering approach was preferred for nanoparticle size distribution testing in an aqueous environment (Powers et al., 2006).

3   Methods

Section 3.1 and 3.2 discuss produced water sampling methods and suspended solid isolation protocols. Detailed methods and underlying principles of particle size measurement and X-ray photoelectron spectroscopy (XPS) are discussed in Sections 3.3 and 3.4. A complete method description also is provided in the method section of Chapter 4.

3.1   Sampling methods

Two Noble Energy Inc. well pads were studied: Crow Creek (CC) and Chandler State (CS), both located in the Wattenberg field of Northern Colorado. Five wells were selected from these two pads, and water samples were collected from each well after flowback started. Sampling schedule is summarized in Table 3-1. It should be noted that not all samples collected were tested in this study for particle size and XPS.

Table 3-1. Sampling Schedule from wells in Crow Creek and Chandler State Pads

Pad	Sampling frequency				
	8 hours	12 hours	24 hours	3 days	7 days
Crow Creek	Day 1 to 2	Day 3 to 5	Day 6 to 15	Day 16 to 24	Day 25 to 37
Chandler State	N/A	N/A	Day 1 to 14	Day 15 to 29	Day 30 to 50

Samples were collected at the wellhead during the first few days after production when all flowback fluids were separated at the temporary oil-water separator and, after the permanent production separator was installed, samples were collected from the service valve post-separation. For the Crow Creek and Chandler State pads, the production separator was installed five and four days, respectively, after flowback started.

Figure 3-1 illustrates the sampling method at the wellhead. Oil-water mixed fluid was collected in a five-gallon carboy and allowed to settle for 15 minutes. Produced water then was separated from crude oil through the lower spigot. When the production separator was in operation, samples were collected post oil-water separation from a service valve (Figure 3-2).

Figure 3-1. Sample collection from wellhead

Figure 3-2. Sample collection from production separator

3.2   Suspended Solids Isolation Procedures

To better capture suspended solids in produced water for XPS elemental test, a solids

separation protocol was developed. The main objective of this procedure is to capture most

suspended solids as well as to prepare the sample to be ultra-high-vacuum (UHV) compatible for

the XPS test. Some extra steps also were also designed and applied to eliminate possible

interferences. For example, because the glass fiber filter could possibly contribute interfering

silicon signals in the XPS test, a silver filter was used. Further, because the sample could be

contaminated by organic carbon through previously applied experiment procedures, the sample

was burned at 550 ˚C immediately before the XPS scan.

The following preparation steps, illustrated in Figure 3-3, were applied:

(1) 50mL of water sample were added to a flat crucible and dried at 105 ˚C and then burned at

550 ˚C in a muffle furnace. To collect enough solid, 200- mL of each sample were added to each

of four crucibles.

(2) Residuals were collected and ground into a fine powder.

(3) Fine powder from Step 2 was dissolved into 200 mL of deionized water with a magnetic

stirrer.

(4) The mixed solution was filtered through a 0.2-μm silver filter (Sterlitech Corp. WA) under

vacuum.

(5) The filter was then rinsed with 200 mL deionized water to wash off dissolved salts.

(6) The filter was furnaced again at 550 ˚C, and the sample was tested by XPS within one hour.
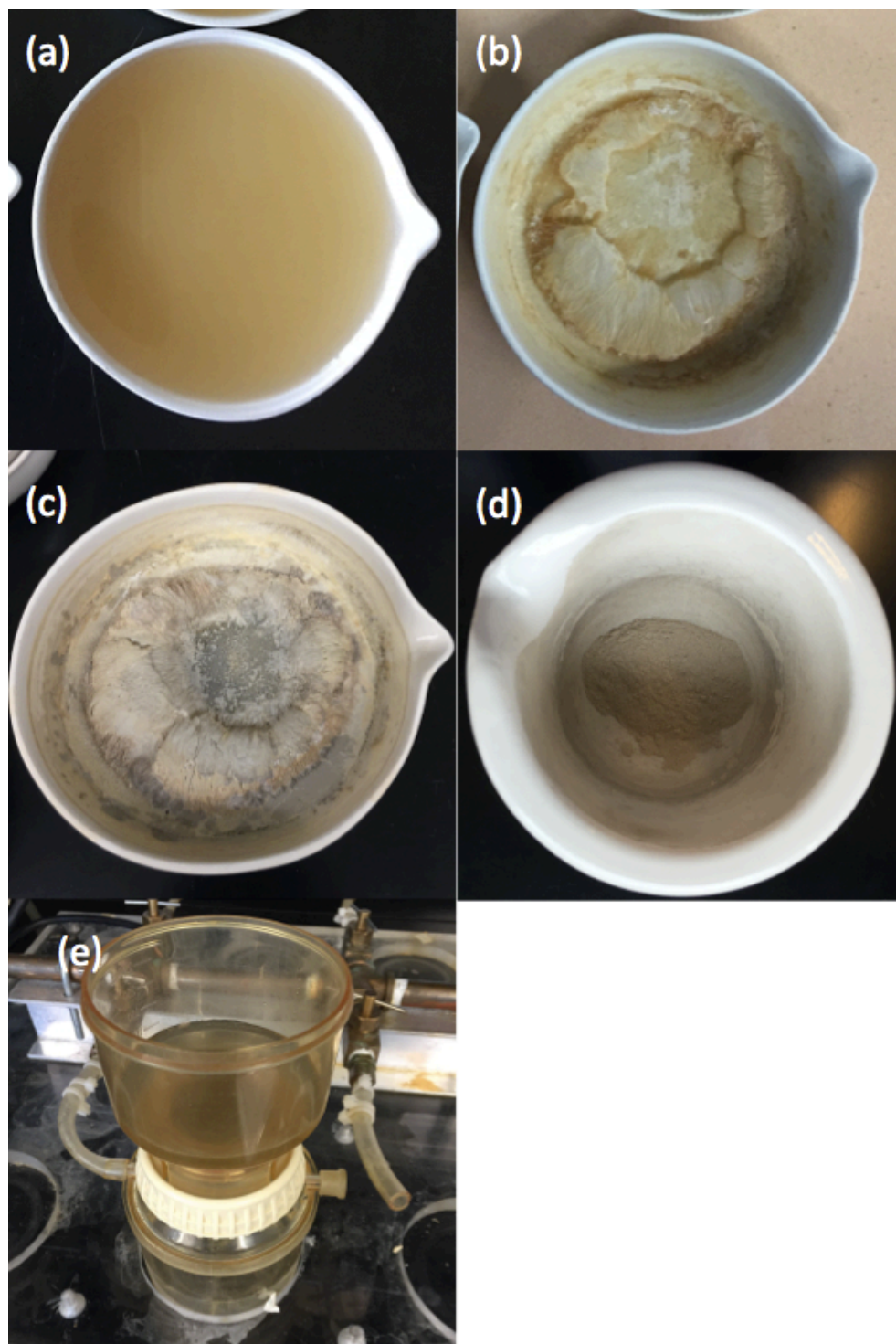
Figure 3-3. Suspended solid isolation steps: (a) raw produced water added to the flat crucible; (b) dried at 105 °C; (c) burned at 550 °C; (d) ground into fine powder; (e) filtered through 0.2-μm silver filter.

3.3   Particle Sizing

Particle size and particle size distribution (PSD) are the key properties describing colloidal and dispersed systems. In this study, a dynamic light scattering (DLS) method was applied to size particles, using a 90-Plus Particle Size Analyzer (Brookhaven Instruments, NY) at a fixed, scattering angle of 90° and temperature of 25 °C (Figure 3-4).
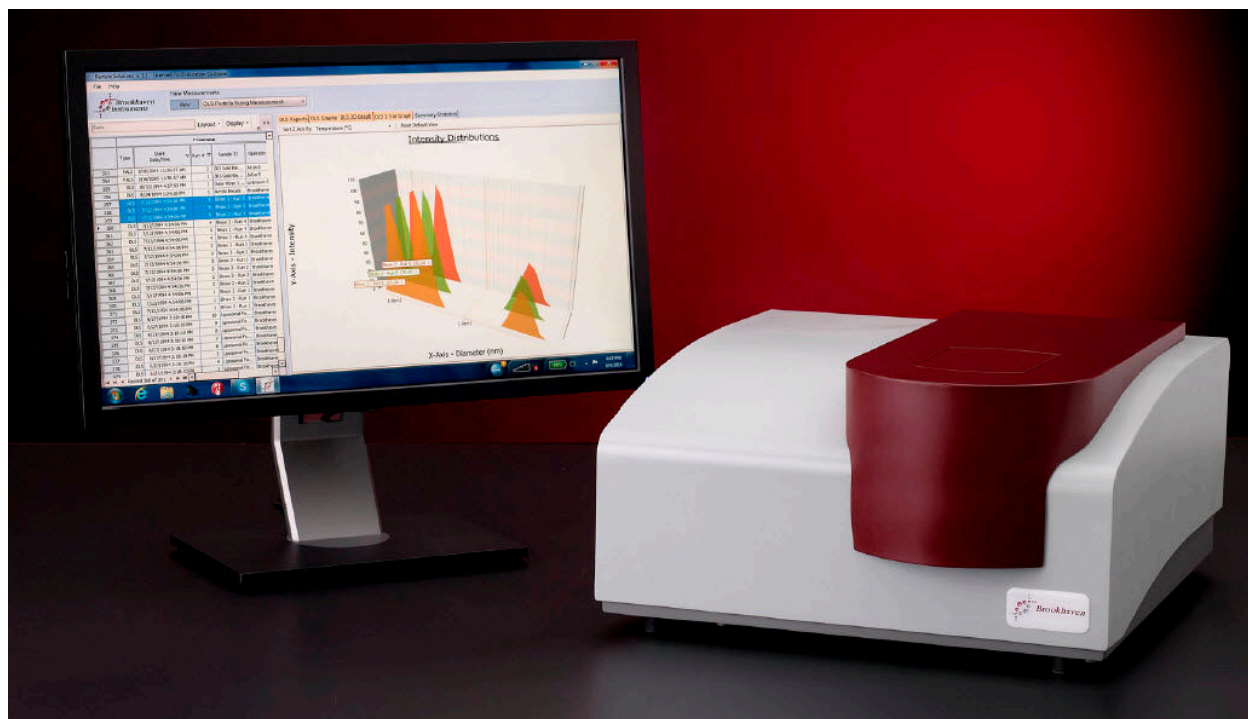

Figure 3-4. Brookhaven Instruments 90-Plus Particle Size Analyzer

(brookhaveninstruments.com)

DLS is one of the most widely applied techniques for colloidal system study, and it provides fast, accurate, and reliable results (Bryant & Thomas 1995). When a beam of monochromatic laser light hit particles in solution, the light scatters in all directions—an effect also known as Rayleigh scattering. As the scattering intensity fluctuates over time, Brownian

motion of the particle is measured; assuming particles moving independently from each another, the hydrodynamic diameter d can be deduced from the Stokes-Einstein equation:

$$D = \frac{k_B T}{3\pi\eta d}$$

Where,

D = transitional diffusion coefficient;

k_B= Boltzmann's constant (1.38×10^{-23} m^2 kg s^{-2} k^{-1});

T = temperature (K);

η = solution viscosity (Pa s);

d =hydrodynamic diameter.

Because particle sizes are determined by the observation of particle motion, the diameter obtained by DLS method is "the diameter of a sphere that has the same translational diffusion coefficient as the particle" (Malvern Instruments, 2012). Specifically, the translational diffusion coefficient depends on the core size of the particle, surface structures and concentration and type of ions in the dispersion system.

Two models are available for the representation of PSD: the Lognormal Size Distribution (LSD), and the Multimodal Size Distribution (MSD). The LSD model provides a simplified approach that assumes a single log normal distribution with only one unified size distribution peak generated. The MSD model, however, uses a Non-Negatively constrained Least Squares (NNLS) algorithm to fit the data, an approach that offers more information about the presence of different sizes of particles and the relative intensity of different-size groups (Brookhaven Instruments Inc., 1995; Beliciu & Moraru, 2009). Figure 3-5 provides a simple comparison of LSD and MSD.
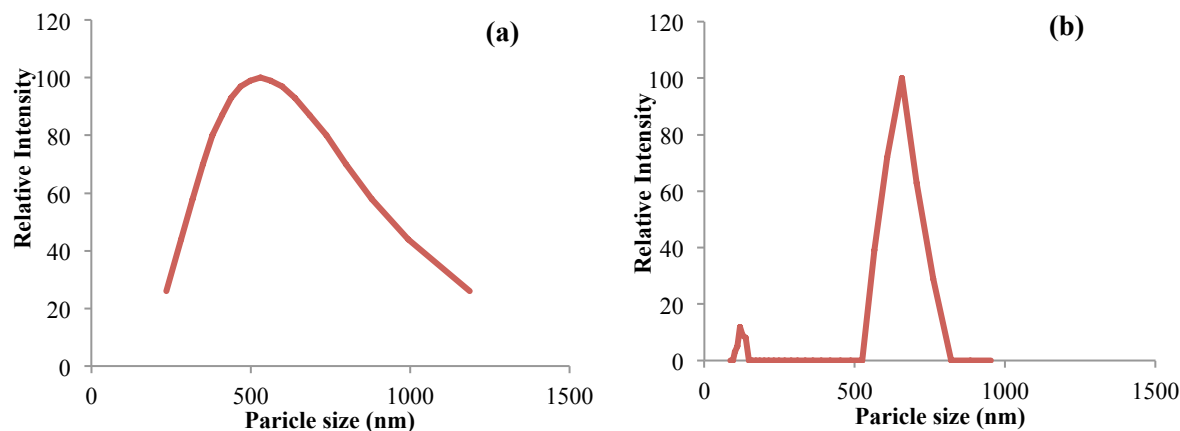
Figure 3-5. Different representation models for particle size distribution of study sample CC73-1-Day 1: (a) Lognormal Size Distribution (LSD) and (b) Multimodal Size Distribution (MSD)

The MSD model is more accurate in representing different size groups and serves as a more appropriate approach within the context of suspended solids characterization in produced water. Accordingly, the MSD algorithm was selected to represent particle size distribution; in this study, the results of three runs were averaged to calculate the apparent hydrodynamic diameter of particles.

3.4   X-ray Photoelectron Spectroscopy

X-ray photoelectron spectroscopy (XPS) is a surface-sensitive, semi-quantitative technique that measures the elemental composition of a sample—typically a powder sample. An empirical formula and chemical state can be deduced from the binding energy shift and relative intensity through high-resolution scans of selected elements.

A typical XPS system, shown in Figure 3-6, consists of three parts: a monochromatic X-ray source, electron energy analyzer, and a detector (Haasch, 2014). The X-ray source generates a beam of incident photons with energy hυ and, when an atom absorbs an X-ray photon, a

photoelectron is emitted with a kinetic energy of E_K. The detector then measures the emitted

kinetic energy E_K. The unique binding energy specific to each element can be calculated by:

$$E_B = h\upsilon - E_K - W$$

Where $h\upsilon$ is the photon energy (for a Al Kα X-ray source, $h\upsilon$=1486.6 eV); E_K is the kinetic

energy of the electron; and W is the spectrometer work function. These three parameters are

either known or measurable; these values allow the binding energy to be derived easily
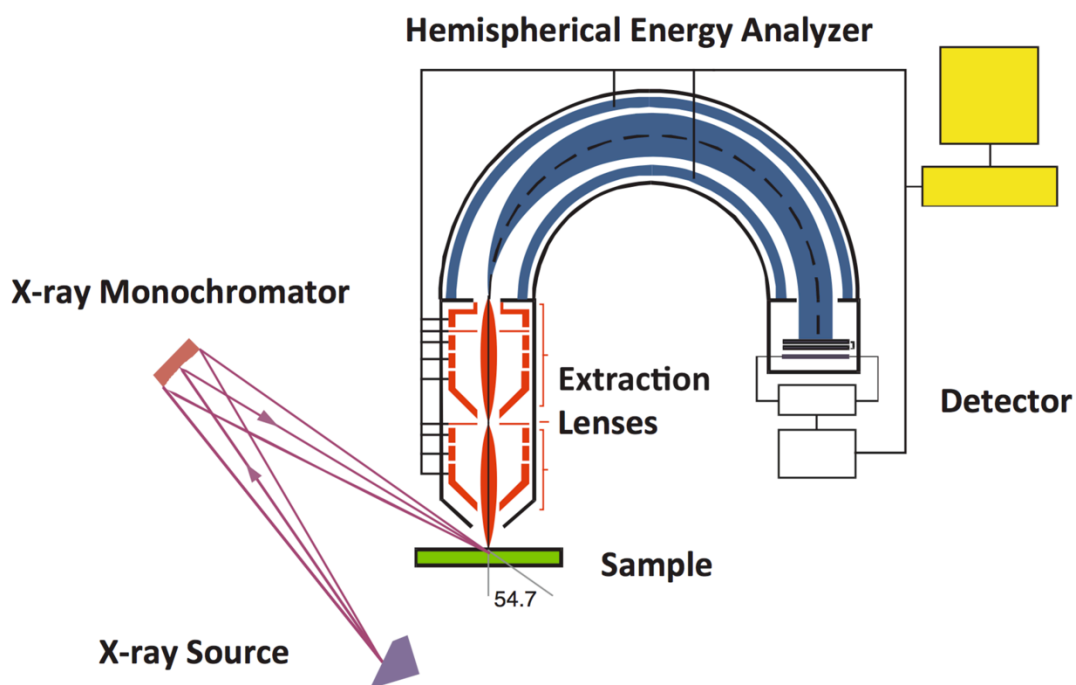
Figure 3-6. Schematic of a typical, modern high resolution X-ray photoelectron spectrometer

(Haasch, 2014)

The surface chemistry of isolated suspended solids samples was analyzed by a PEI-5800

XPS-Auger spectrometer (Physical Electron, MN) at the Central Instrument Facility (CIF),

Colorado State University (Figure 3-7). The PEI-5800 system was equipped with a

monochromatic Al Kα X-ray source ($h\upsilon$=1486.6 eV) and operated at an ultra-high vacuum
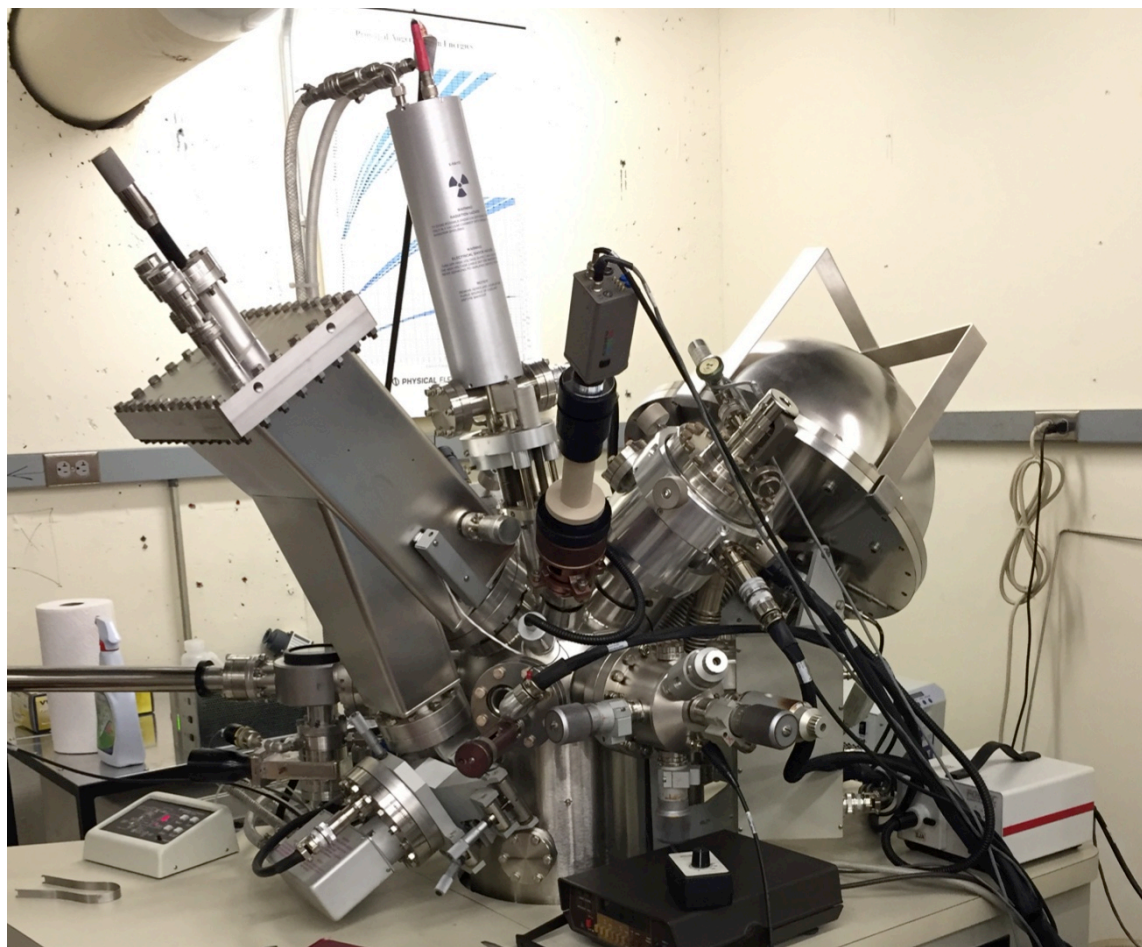
pressure greater than 10^{-8} Torr.

Figure 3-7. PEI-5800 XPS-Auger spectrometer system

Measurements were taken at a photoelectron takeoff angle of 45° relative to the surface plane. Ten surveys were scanned over the range of 0-1100 eV, at a resolution of 1 eV. High-resolution spectra of selected element were acquired at a pass energy of 23.5 eV and a step- size of 0.1 eV.

Binding energies were referenced to the C1s line of adventitious hydrocarbon at 284.8 eV. XPS peak 4.1 software was used to fit the core level XPS spectra: line shape was fitted with a Lorentzian-Gaussian ratio of less than 20 percent, and the full width at half-maximum

(FWHM) was referenced with literature values or set to lower than 2 for an automatic

approximation.

4 Journal Article

Summary

Water management is a central issue in oil and gas development. Hydraulic fracturing applied in unconventional tight oil and gas development requires large amounts of water, and the disposal of the waste stream returning to the surface has raised significant public health and environmental concerns. The wastewater that results after production contains high levels of organic and inorganic matters, and the beneficial reuse of produced water requires some level of treatment to remove emulsified oil and grease, suspended solids, and multivalent ions that could cause potential scale or clogging problems in future application. It is critically important to identify the quantity and makeup of solids in produced water, so that optimized reuse or treatment approach can be achieved.

This study targeted the qualitative and quantitative characterization of solids in produced water from oil and gas operations, with the purpose of identifying the difference in solids from wells fractured with fresh water and those fractured with recycled water. Samples were collected from five wells at the Crow Creek and Chandler State pads in the Wattenberg field of Northern Colorado. Gravimetric analyses of dissolved and suspended solids were performed and particle size distributions were measured. Suspended solids also were isolated and characterized with X-ray photoelectron spectroscopy (XPS).

Gravimetric analyses showed that total dissolved solids (TDS) averaged about 24000 mg/L and 17000 mg/L for Crow Creek and Chandler State wells, respectively. Total suspended solids (TSS) concentrations were much lower, measuring 550 and 260 mg/L for two pads, respectively. About 9 to 25 percent of TDS was volatile, and volatile portion of TSS were measure from 88 to 99 percent. Particle sizes stabilized at about 400 nm and 900 nm for wells

on the Crow Creek and Chandler State pads, respectively. At the Crow Creek pad, particle sizes were smaller and more uniform in produced water samples collected during the first week of production from the well fractured with recycled water, suggesting that the recycled water was more compatible with shale formation and that wells fractured with recycled water tend to clean out faster. XPS tests for isolated suspended solids showed the presence of major elements such as oxygen, carbon, and silicon, along with minor element such as calcium, magnesium, zirconium, iron, and others. Core-level scanning confirmed that the isolated suspended solids were composed mainly of carbonate-based minerals and metal oxides; several iron compounds with different valences also were found in sample.

Key words: Produced water, Wattenberg Field, solid characterization, particle size, XPS

4.1   Introduction

Oil and gas are main energy sources worldwide. Recent development of technology involving horizontal drilling and hydraulic fracturing offers tremendous potential in unconventional oil and gas production. U.S. production of tight oil has increased dramatically from less than one million barrels per day (MMbbl/d) in 2010 to more than three MMbbl/d in 2013 (EIA, 2014). Hydraulic fracturing of tight shale formations requires a large amount of water, compared to conventional oil and gas production. Goodwin et al. (2013) estimated that each vertical and horizontal well in the Wattenberg field of Northern Colorado uses an average of 0.4 and 2.9 million gallons of water, respectively. With oil-rich fields often located in water-scarce areas, the water demand of oil and gas production could add to the already-intense demand for water for municipal and agricultural purposes or even contribute to water shortages during severe drought conditions.

Large amounts of water are used to deliver the fracturing package under extremely high pressure; this effort opens up fractures within the target formation, and a large portion of co-produced water eventually flows back the with oil and gas product. The transport, treatment, and reuse of this produced water, after it is separated from the crude oil, have become crucial waste management and environment issues. The most common means of disposing wastewater from oil and gas production in the United States is through deep well injection—a practice that costs an average of 1 to 4 U.S. dollars per barrel (Clark and Veil, 2009). However, an increasing number of oil and gas companies are taking advantage of using produced water as a component of fracturing fluid for new wells (Huang et al., 2006); this practice could significantly minimize the demand for fresh water and the transportation and handling costs for deep well injection.

With multiple studies focused on produced water qualities and characterization (Benko and Drewes, 2008; Alley et al., 2011; Barbot et al., 2013), the suspended solids characteristics of produced water and its dispersed system has hardly been investigated. The understanding of solids properties and chemical composition will help guide the selection of the treatment technique that will improve wastewater treatment effectiveness and allow beneficial wastewater reuse. In this study, dissolved and suspended solids of produced water were characterized with gravimetric and particle sizing analyses; suspended solids were captured and surface chemistry was tested through X-ray photoelectron spectroscopy (XPS). The effect of using fresh surface water, compared to recycled produced water, on the resulting produced water qualities was also studied.

Research objectives:

1. To characterize solids, both qualitatively and quantitatively, in produced water flowing back from unconventional wells in oil and gas operations.

2. To compare the difference between solids from wells fractured with fresh water and recycled water.

3. To develop solids isolation and preparation protocols and characterize the solids with X-ray photoelectron spectroscopy (XPS).

4.2   Methods

4.2.1   Sampling Methods

Two Noble Energy Inc. well pads were studied: Crow Creek and Chandler State, both located in the Wattenberg field of Northern Colorado as shown in Figure 4-1. Five wells, described in Table 4-1, were selected from these two pads, and water samples were collected from each well after flowback started. Wells from the same pad were constructed at the same time and parallel to each other.

Table 4-1. Five wells selected for study

Well Name	API #	True vertical depth (ft)	Formation	# of Stages	Frac Fluid Type	Fracturing source water
Crow Creek State AC36-**73HN**	05-123-37423	6,685	Niobrara	20	PermStim	1:7 recycle/fresh
Crow Creek State AC36-**76-1HN**	05-123-37420	6,742	Niobrara	20	PermStim	100% fresh
Chandler State D15-**72-1HN**	05-123-38322	6,750	Codell	23	SilverStim	100% fresh
Chandler State D15-**73-1HN**	05-123-38323	6,750	Codell	23	SilverStim	1:7 recycle:fresh
Chandler State D15-**74-1HN**	05-123-38321	6,750	Codell	23	SilverStim	1:5 recycle:fresh
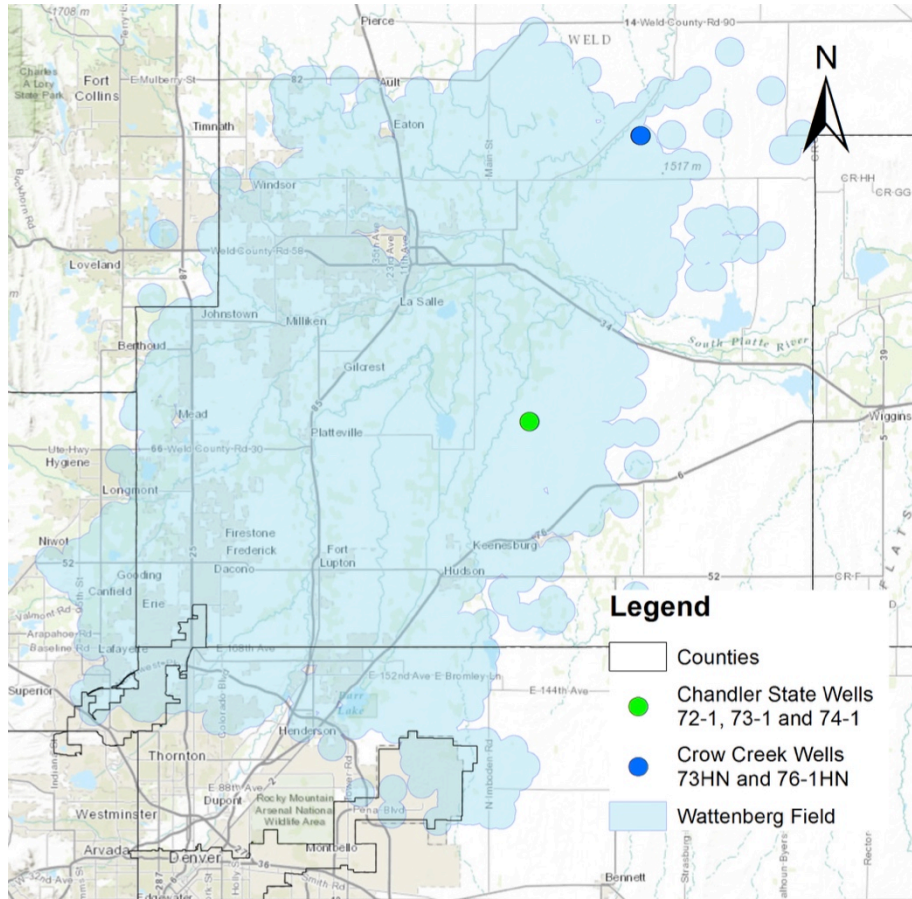
Figure 4-1. Location of wells within the Chandler State and Crow Creek pads

4.2.2 Gravimetric analyses and produced water quality

Gravimetric analyses of solids were conducted according to Standard Method 2540 (APHA, 1995). Samples for total solids (TS), total dissolved solids (TDS), and total suspended solids (TSS) determination were dried at 105 °C; samples collected for total volatile solids (TVS), volatile dissolved solids (VDS), and volatile suspended solids (VSS) determinations were muffled at 550 °C. Whatman 934-AH glass microfiber filters (1.5-μm equivalent pore size) were used to filter samples. Metal and ion concentrations also were determined for reference. Ion

concentration data were collected from Nalco Champion (Ecolab USA Inc.) and eAnalytics

Laboratory (Loveland, CO) for Crow Creek wells and Chandler State wells, respectively.

4.2.3   Particle Sizing

Particle size and particle size distribution (PSD) are the key properties describing

colloidal and dispersed systems. In this study, a dynamic light scattering (DLS) method was

applied to size particles, using a 90-Plus Particle Size Analyzer (Brookhaven Instruments, NY) at

a fixed, scattering angle of 90° and temperature of 25 °C.

A multimodal size distribution (MSD) algorithm was used to represent particle size distribution

(PSD); the results of three runs were averaged to calculate the apparent hydrodynamic diameter

of particles.

4.2.4   X-ray Photoelectron Spectroscopy (XPS)

The surface chemistry of isolated suspended solids samples was analyzed by a PEI-5800

XPS-Auger spectrometer (Physical Electron, MN) at the Central Instrument Facility (CIF),

Colorado State University. The PEI-5800 system was equipped with a monochromatic Al Kα X-

ray source (hv=1486.6 eV), and operated at an ultra-high vacuum pressure greater than 10^{-8} Torr.

Measurements were taken at a photoelectron takeoff angle of 45° relative to the surface plane.

Ten surveys scanned over the range of 0-1100 eV, at a resolution of 1 eV, were averaged. High-

resolution spectra of selected element were acquired at a pass energy of 23.5 eV and a step- size

of 0.1 eV. Binding energies were referenced to the C1s line of adventitious hydrocarbon at 284.8

eV. XPSPEAK 4.1 software was used to fit the core level XPS spectra.

To better capture suspended solids in produced water for XPS elemental testing, a solids

separation protocol was developed. The following preparation steps were applied: 1) 200 mL of

water sample was dried at 105 ˚C and then burned at 550 ˚C in a muffle furnace; residuals were

33

ground into a fine powder; 2) the fine powder was dissolved into 200 mL of deionized water with a magnetic stirrer; 3) the mixed solution was filtered through a 0.2-μm silver filter (Sterlitech Corp. WA) under vacuum; 4) filter was then rinsed with 200 mL deionized water to wash off dissolved salts; 5) the filter was furnaced again at 550 ˚C and the sample was tested by XPS within one hour to prevent possible organic carbon contamination through air exposure.

4.3 Results and Discussion

4.3.1 Produced Water Quality and Solids Distribution

Table 2 summarizes the water quality of Crow Creek and Chandler State wells. While metal ions such as calcium, magnesium, iron, strontium, and zirconium were present, sodium chloride was found to be the dominant salt in both well pads. Sample pH averaged approximately 7.5, and sample buffer capacity was relatively high--suggesting that a significant amount of acid or base might be required for softening, if treatment was deemed necessary. Water quality was found to vary considerably from well to well, and organic and inorganic constituent concentrations of samples from Crow Creek wells were nearly all considerably higher than those of samples from Chandler State wells. Specifically, TOC and DOC levels of Crow Creek samples were twice as high as those measured in samples collected from the Chandler State wells. Average TDS measured in Crow Creek well samples was 40 percent higher than that found in Chandler State well samples. The sulfate concentration averaged 368 mg/L and 29 mg/L in samples from Crow Creek wells and Chandler State wells, respectively. Because sulfate forces the precipitation of barium, barium was the only parameter found to be lower in the Crow Creek well samples. Overall, the characteristics of inorganic constituents in produced water are primarily inherited from the rock formations with which the water had

contact (Benko and Drewes, 2008). Consequently, the difference in inorganic constituent-related water quality between the wells is due, in part, to the geologic variations within the Wattenberg field.

Table 4-2. Water Quality Summary for Crow Creek and Chandler State Wells

Wells		Crow Creek wells 73 and 76-1			Chandler State wells 72-1, 73-1 and 74-1		
Number of samples		60 Samples collected from day 1-54			69 Samples collected from day 1-71		
Parameters		Minimum	Maximum	Average	Minimum	Maximum	Average
pH		6.6	9.1	7.5	6.2	9.0	7.4
Cond.	(mS/cm)	0.9	52.9	20.8	14.6	44.1	23.8
TOC	(mg/L)	362	12,170	4,320	80	4,845	2,038
DOC	(mg/L)	366	11,930	3,079	87	2,125	1,477
Alkalinity	(mg/L as CaCO$_3$)	234	2,264	1,301	432	1,488	975
TS	(mg/L)	1,540	38,940	25,638	9,020	40,060	17,333
TDS	(mg/L)	1,420	33,760	24,357	12,880	25,620	16,955
TSS	(mg/L)	21	1,542	550	44	1,229	257
TVS	(mg/L)	360	17,880	5,469	940	24,480	3,985
VDS	(mg/L)	340	10,940	4,250	780	5,420	3,384
VSS	(mg/L)	4	1,524	516	23	1,208	239
Al	(mg/L)	0.1	16.0	5.4	0.1	1.4	0.6
B	(mg/L)				5.0	20.4	15.3
Ba	(mg/L)	0.1	5.6	2.1	1.5	15.5	6.4
Br	(mg/L)				25	51	35
Ca	(mg/L)	43	435	269	54	186	104
Cu	(mg/L)	0.0	0.4	0.1			
Fe	(mg/L)	4.2	171.1	44.0	0.5	60.4	29.8
K	(mg/L)				40	3,399	120
Mg	(mg/L)	21.3	57.7	37.1	7.5	25.1	14.9
Na	(mg/L)	107	10,199	5,553	2,339	7,156	4,384
Si	(mg/L)				4	60	45
Sr	(mg/L)	0.1	60.4	31.9	7.7	31.6	16.5
Zn	(mg/L)	0.0	0.8	0.1	0.2	6.7	0.9
Cl	(mg/L)	163	15,712	8,458	4,980	10,800	7,072
NH$_4$	(mg/L)				10	130	21
HCO$_3$	(mg/L)	63	3,660	1,190	512	1,476	955
SO$_4$	(mg/L)	316	446	368	1	268	29

Figure 4-2 details the volatile portion of each solids category. About 13 to 46 percent of TS, and 9 to 25 percent of TDS, were volatile, indicating that a large amount of organic compounds were present in the produced water. TSS also was found to be highly volatile, ranging from 88 to 99 percent. During TSS determination, a large amount of emulsified oil was caught on the filter when isolating suspended solids--likely the reason why such a high volatile percentage of suspended solids was recorded. Given the organic-rich nature of produced water, a new suspended solids isolation protocol was established for better performance in XPS testing, as discussed in Methods Section 4.2.4.

	CC 73 Day 6	CC 73 Day 21	CC 76-1 Day 6	CC 76-1 Day 21	CS 72-1 Day 6	CS 72-1 Day 20	CS 73-1 Day 6	CS 73-1 Day 20	CS 74-1 Day 6	CS 74-1 Day 20
TS %volatile	21%	24%	46%	13%	37%	21%	28%	21%	25%	19%
TDS %volatile	17%	12%	25%	9%	30%	25%	23%	20%	22%	18%
TSS %volatile	98%	99%	98%	97%	98%	88%	97%	93%	95%	96%
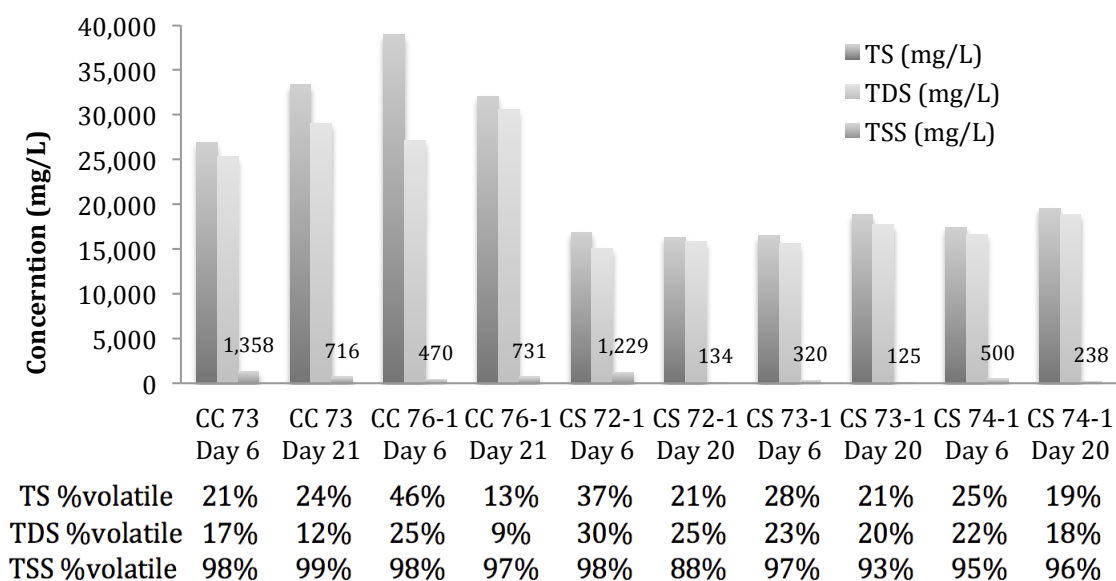
Figure 4-2. Solids distribution for Chandler State wells on Day 6 and Day 20 and Crow Creek wells on Day 6 and Day 21. The lower table summarizes the volatile portion of solids in each category.

Consistent TDS values were found within the same pad, suggesting that fracturing wells with some portion of recycled water might not necessarily lower the produced water quality with respect to inorganic constituents. As discussed above, effluent TDS concentrations are most

likely influenced by the brine and salt layer of the shale formation itself, and not by the water quality of fracturing source water.

4.3.2 Particle Size Distribution

Particle size and particle size distribution (PSD) are the key properties of colloidal and dispersed systems. Solids in produced water represent a wide range of materials, including formation solids, corrosion and scale products, bacteria, waxes, and asphaltenes (Fakhrul et al., 2009). Effective particle diameter, illustrated in Figure 4-3, represents an average size of the particles in the sample. Higher particle sizes were measured in the preflow and Day 1 samples, but that trend flattens out soon after production. Large particles observed during the early-production period might have originated from clay content in the shale formation and/or the fracturing package (crosslinking gel, sand proppant, etc.). PSD profiles presented in Figure 4-4 show that early flowback samples contained a large variety of solids with particles ranging from 100 to 10,000 nm. As the high pressure of hydraulic fracturing dropped after production, fractures tended to close up enough to block the passage of larger particles. Once particle size stabilized, measurements showed the Chandler State wells had larger particle sizes than the Crow Creek wells. Particle sizes in Crow Creek pad samples stabilized at about 100 to 200 nm; most particles measured in Chandler State pad samples were greater than 400 nm in the first 20 days. However, during the first week of production, the Crow Creek well fractured with fresh water--well CC-76-1--was found to have larger particle sizes than the well fractured with recycled water (CC-73).
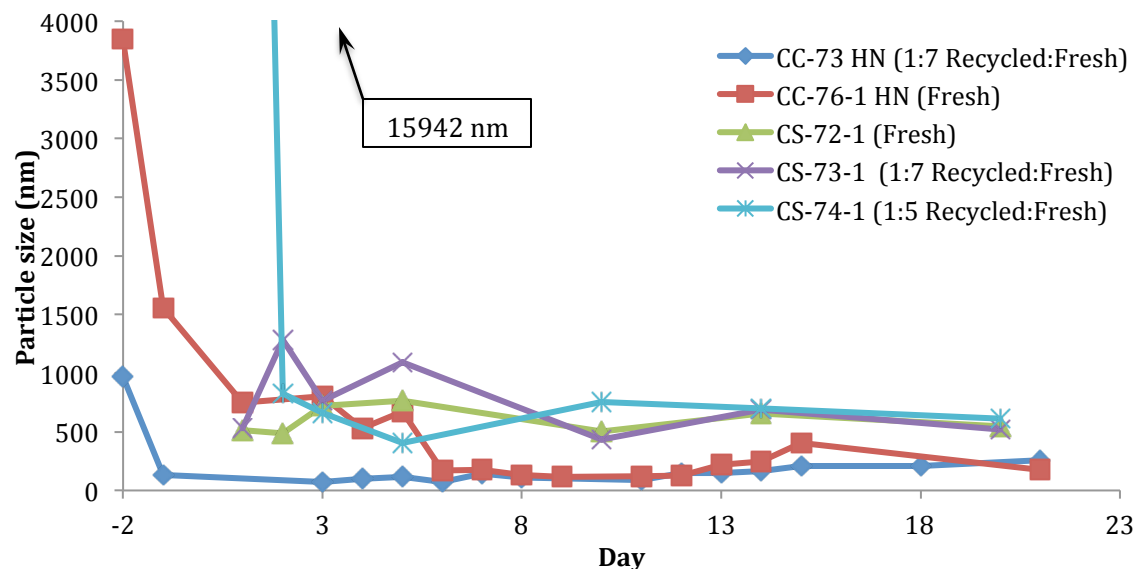
Figure 4-3. A summary of effective particle sizes for Crow Creek and Chandler State wells (Day -2 and Day -1 day represent the pre-flow period before production, and Day 1 refers to the production day.)

Figure 4-4 illustrates the different PSD patterns between well CC-73 and CC-76-1: well 76-1 particles showed a broader peak width and multiple peaks of size distribution, compared to well 73 that showed a smaller particle size and a uniform mono distribution peak after production. In general, CC-73 had smaller particle sizes and tended to clean out much faster than well CC-76-1. One theory is that recycled water has higher salinity and is more compatible with shale formation; therefore, the mineral solubility equilibrium and chemical equilibrium can be established much faster. Yet, similar effects were not found in early Chandler State well samples, other than the extremely high particle size recorded in CS-74-1 Day 1 sample, in which tiny black particles could be seen floating. Later XPS testing suggested these particles could be iron oxides.
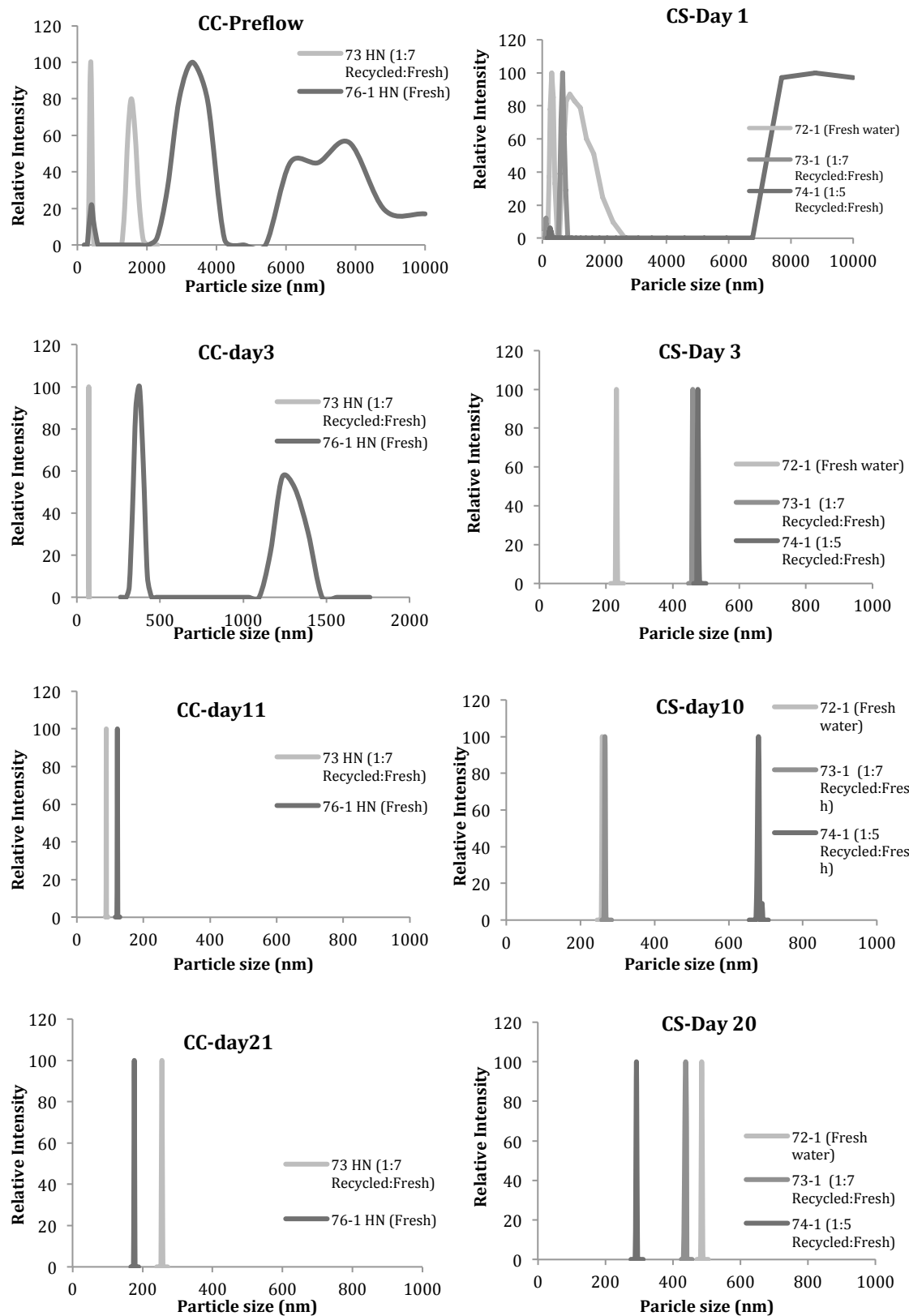
Figure 4-4. Particle size distribution (PSD) for Crow Creek and Chandler State wells

4.3.3 X-ray Photoelectron Spectroscopy (XPS)

Analyzing the XPS spectra of peaks at different levels of binding energy allowed all elements present in the solid samples to be identified; the full list of elements and relative atomic percentages is presented in Table 4-3. For oxygen, carbon, silicon and magnesium, detailed temporal trends are provided in Figure 5.

Table 4-3.Atomic Percentage of All Elements for Chandler State Wells 72-1 HN, 73-1 HN and 74-1 HN, from Day 1 to Day 20 of production

Well No.	CS 72-1 HN					CS 73-1 HN					CS 74-1 HN				
Day	1	2	6	10	20	1	2	6	10	20	1	2	6	10	20
Oxygen	58.3	53.4	60.4	49.7	52.2	58.5	43.2	56.8	58.1	56.2	63.9	44.5	55.3	56.8	62.5
Carbon	6.6	13.2	6.2	16.2	10.4	6.7	13.1	5.8	6.2	4.1	4.1	11.8	8.6	5	5.9
Silicon	12.1	10.9	14.6	9.3	15	12.5	9.3	14.6	9	11.2	6.5	7.7	14.5	13.4	11.9
Calcium	3.6		1.4	2.8	5.1			2.6	4	2.9	7.1	2.8	3.7	2.8	1.8
Magnesium	1.5	3.8	1.3	3.1	3.1	3.6	18.2	4.3	4.5	5.7	10.1	15.5	5	5.2	5.6
Zirconium	1.7	2.7	1.3	0.7		1.8	2.3	1.2	0.9	1		2.3	0.8	1	1
Iron	2.5	1.8	1.6	1.5	4.1	2.3	1.9	1.7	2.3	2.9	2.9	1.2		1.6	3.5
Iodine		0.6		3.9	2.1		2.4	1.5	0.5	4.6		1.8	0.6	2	
Sodium	12.8	11.9	12.2	7.5	5.0	14.6	7.5	9.1	12.7	7.1	0.9	8.4	8.4	10	5.6
Chlorine	1	0.9	0.4	0.9			0.6	1	1.3	1.1		0.9	1.1	1	1.1
Nitrogen			0.6	2.1								1.6	1.3		
Barium										0.1		0.2	0.2		0.1
Silver		0.7		2.2	3		1.5	1.4		3.1		1.4	0.5	1.2	
Sulfur											2.7				
Strontium									0.5						
Phosphorus											1.8				

The data in Table 4-3 show that the most abundant element was oxygen, with an atomic percentage of 40 to 60 percent, followed by carbon and silicon. Because solid samples were burned at 550 ˚C, as described in the preparation procedures detailed in the Methods section of this paper, only inorganic carbon was expected to remain in the residuals. It can be deduced that major chemical components were calcium/magnesium, carbonate mineral, and quartz/clay.

Figure 4-5 shows all three wells followed similar temporal trends in atomic percentage of oxygen and silicon. Magnesium spiked at Day 2 in wells CS-73-1 and CS-74-1, fractured with recycled water, and their atomic percentages were continuously higher than those of well CS-72-1 fractured with fresh-source water. Iron presence was constant at about 2 to- 3 percent of atomic percentage; divalent ions such as barium and strontium were detected only sporadically. The relative abundance of zirconium (Zr) peaked at Day 2 in all three wells. Since Zicronium is generally considered insoluble in crustal fluids and only trace amounts of Zr-bearing mineral are found in shale formations (Werne et al., 2002; Odoma et al., 2015), Zr detected in produced water more likely originates from the cross-linker in the fracturing package. The zirconate-based cross-linker can link polymer molecules together; therefore, it increases the viscosity needed to open up fractures and deliver proppants into the target pay zone. As polymer gel is broken down, Zr is expected to be released and gradually cleaned out from the well bore. Temporal trend of Zr showed this break-down/clean-out process occurred quickly: the relative abundance of Zr decreased after Day 2 for all three wells. Silver spectra were identified occasionally because silver filters were used in this study; the use of silver filters was meant to eliminate interference of silicon spectra that might occur when using fiberglass filters.
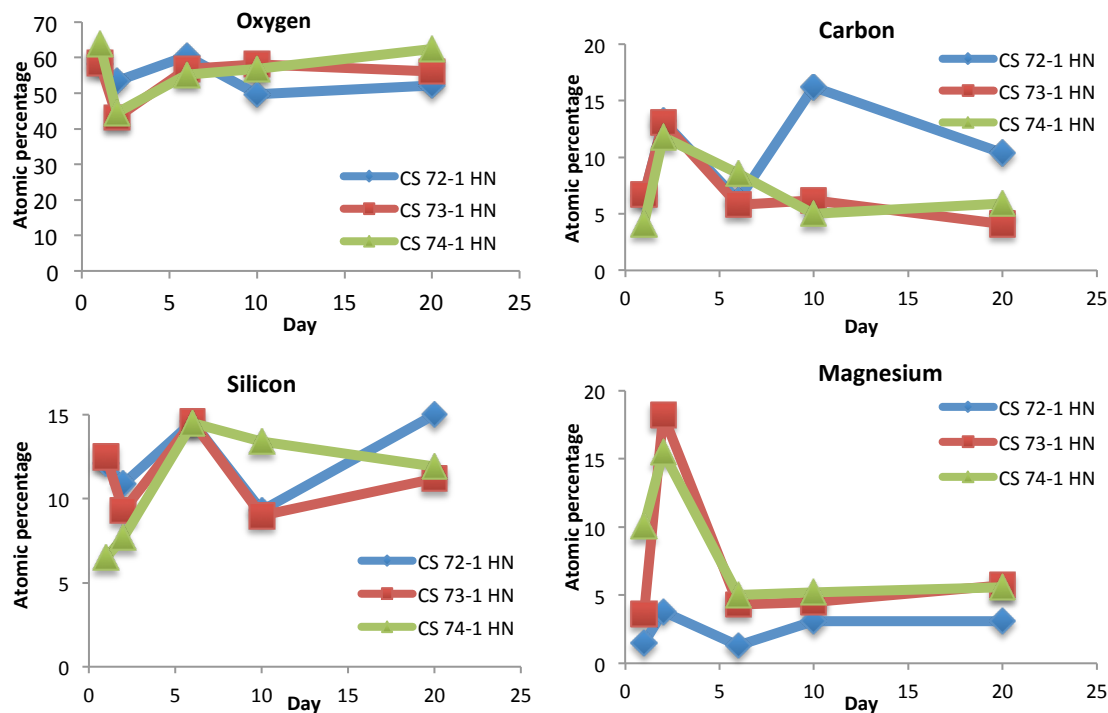
Figure 4-5. Temporal trending of oxygen, carbon, silicon and magnesium in samples from Chandler State wells 72-1 HN, 73-1 HN and 74-1 HN, from Day 1 to Day 20 of production.

Figure 4-6 presents XPS core-level spectra on selected elements. Core-level XPS of carbon and oxygen confirm that most of the suspended solids were composed of carbonate-based minerals and metal oxides. Multivalent iron species were identified, and Fe $2p_{3/2}$ XPS spectra were fitted into three peaks at 710.2, 711.6, and 713.4 eV for Fe_3O_4, Fe_2O_3 and K_2FeO_4, respectively (Deng et al., 2009).
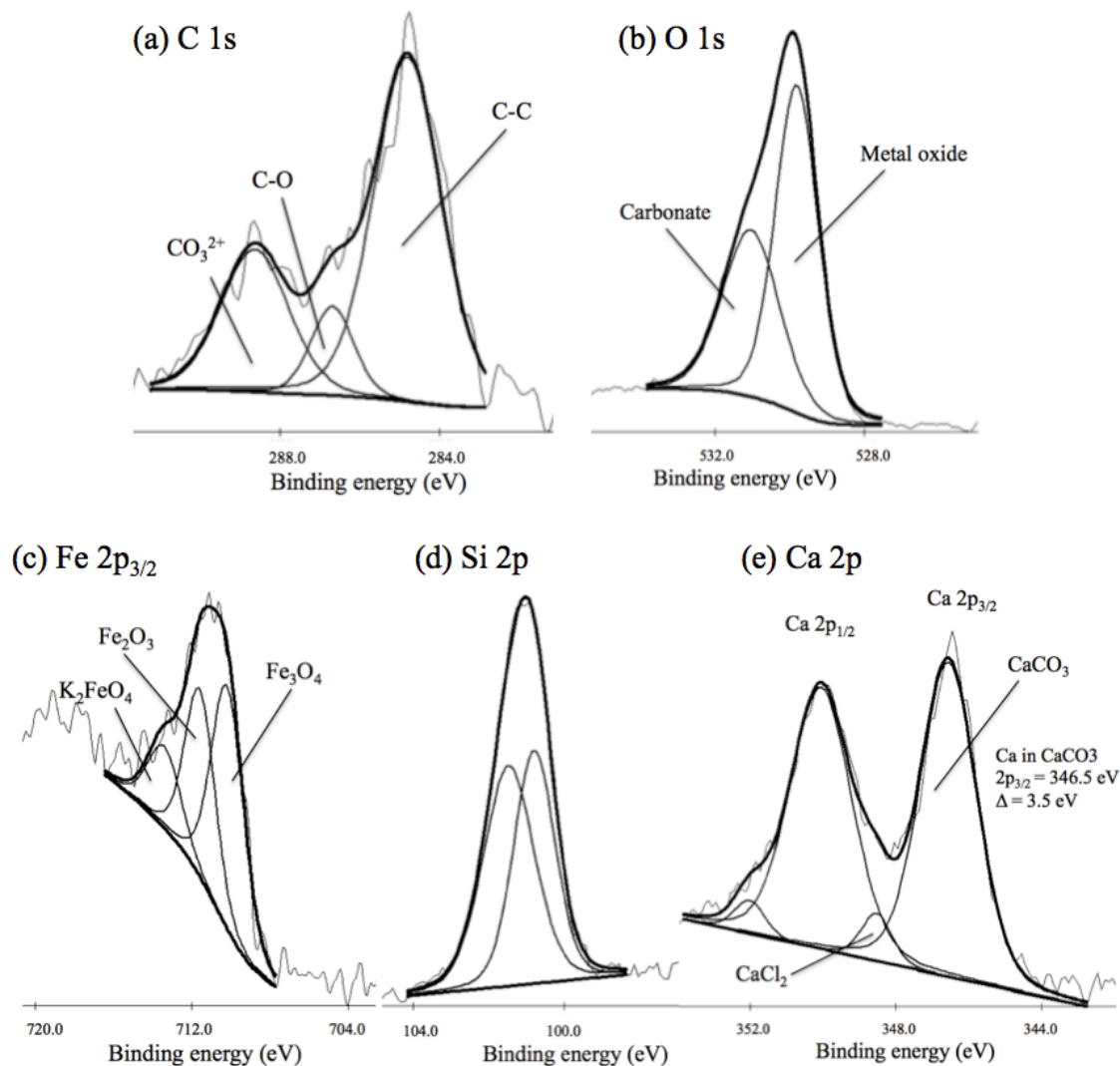
Figure 4-6. Core-level XPS spectra for isolated suspended solids from well CS 72-1 at Day 20:

(a) C 1s, (b) O 1s, (c) Fe 2p$_{3/2}$, (d) Si 2p and (e) Ca 2p

As discussed previously, silicon is expected to be associated with silicate minerals. However, the high-resolution XPS spectra of silicon showed peaks at 100.8 and 101.5 eV that did not match reference binding energy values for silica or silicate at around 103 eV. The 100.8 and 101.5 eV peaks measured represent, instead, SiC and Si$_3$N$_4$, respectively (Parrill & Chung, 1991). Nevertheless, SiC and Si$_3$N$_4$ are highly unlikely to be present in suspended solids in

produced water. Silicon carbide and silicon nitride are rarely found in terrestrial mineral environments (Di Pierro et al., 2003), and natural occurrences are reported primarily in meteorite cases. A possible explanation for this lower binding energy shift could be that silica or silicate was bonded with metal ions. For example, Vempati et al. (1990) discovered that, when ferrihydrite co-precipitated with silica, the binding energy of silicon was shifted lower to 100.8 eV. Moreover, a study done by Gonzalez-Elipe et al. (1988) showed that, in the phyllosilicate minerals framework, substitution of Al or Mg for Si conferred net negative charge to the tetrahedral sheet, thus lowered the photoelectron binding energies of silicon and oxygen. While these are possible explanations, the complex nature of solids isolated from produced water make it difficult to determine its exact chemical composition.

Figure 4-6(e) shows the Ca 2p spectra. The main component at the binding energy of 346.5 eV was attributed to $CaCO_3$, while a smaller peak at 350 eV can be assigned to $CaCl_2$ (Demri& Muster, 1995). The spin orbit splitting between Ca $2p_{3/2}$ and Ca $2p_{3/2}$ was found at 3.5 eV, which also matched literature values (Chastain & King,1992; Demri& Muster, 1995).

4.4 Conclusions

Suspended solids were successfully isolated and characterized by gravimetric analysis, particle sizing, and XPS. Gravimetric analyses showed that dissolved and suspended solids concentrations were similar for wells in the same pad. Major differences were found between the wells fractured with fresh water and recycled water with respect to particle size and PSD during the first week of production. The smaller and mono-distribution of particle size identified suggests that recycled water is more compatible with shale formation and that wells fractured with recycled water clean out faster. XPS tests confirmed the presence of major elements,

including oxygen, carbon, and silicon, and some minor elements such as calcium, magnesium, zirconium, iron, and others. Core-level scanning confirmed that the isolated suspended solids were composed primarily of carbonate-based minerals and metal oxides; several iron compounds with different valences were also found in these samples.

5 Reference

APHA (1995). Method 2540. Total, fixed, and volatile solids in solid and semi-solid samples. In: Standard Methods for the Examination of Water and Wastewater, 19th Ed. American Public Health Association, Washington, DC, USA. pp. 2-58.

Alley, B., Beebe, A., Rodgers, J., & Castle, J. W. (2011). Chemical and physical characterization of produced waters from conventional and unconventional fossil fuel resources. Chemosphere, 85(1), 74-82.

Acharya, H. R., Henderson, C., Matis, H., Kommepalli, H., Moore, B., & Wang, H. (2011). Cost effective recovery of low-TDS frac flowback water for re-use. US Department of Energy: Washington, DC.

Azema, N., Pouet, M. F., Berho, C., & Thomas, O. (2002). Wastewater suspended solids study by optical methods. Colloids and Surfaces A: Physicochemical and Engineering Aspects, 204(1), 131-140.

Barbot, E., Vidic, N. S., Gregory, K. B., & Vidic, R. D. (2013). Spatial and temporal correlation of water quality parameters of produced waters from Devonian-age shale following hydraulic fracturing. Environmental science & technology, 47(6), 2562-2569.

Beliciu, C. M., & Moraru, C. I. (2009). Effect of solvent and temperature on the size distribution of casein micelles measured by dynamic light scattering. Journal of dairy science, 92(5), 1829-1839.

Benko, K. L., & Drewes, J. E. (2008). Produced water in the Western United States: geographical distribution, occurrence, and composition. Environmental Engineering Science, 25(2), 239-246.

Birol, F., Corben, J., Argiri, M., Baroni, M., Corbeau, A. S., Cozzi, L., & Yangisawa, A. (2011).

    Are we entering a golden age of gas. IEA World Energy Outlook.

Bishop, R. E.(n. d.). Management of Waste Fluids from Natural Gas Exploration and Production:

    Comparison of New York State and Delaware River Basin Commission

    Regulations. Delaware Riverkeeper Network.

BP Energy (2014). BP Energy Outlook 2035. BP plc, London, United Kingdom. Available

    online: bp.com/energyoutlook (accessed 2015/04/28).

Brookhaven Instruments Inc. (1995). 90Plus/BI-MAS Multi Angle Particle Sizing Option

    Operation Manual.

Bryant, G., & Thomas, J. C. (1995). Improved particle size distribution measurements using

    multiangle dynamic light scattering. Langmuir, 11(7), 2480-2485.

Chastain, J., & King, R. C. (Eds.). (1992). Handbook of X-ray photoelectron spectroscopy: a

    reference book of standard spectra for identification and interpretation of XPS data (p.

    261). Eden Prairie, MN: Perkin-Elmer.

Clark, C. E., & Veil, J. A. (2009). Produced water volumes and management practices in the

    United States (No. ANL/EVS/R-09-1). Argonne National Laboratory (ANL).

Colorado Oil & Gas Association(COGA). (2015) Water Use Fast Facts. (Available online:

    http://www.coga.org/pdfs_facts/WaterUse_Fast_Fact.pdf).

Demri, B., & Muster, D. (1995). XPS study of some calcium compounds. Journal of materials

    processing technology, 55(3), 311-314.

Deng, S., Yu, G., Chen, Z., Wu, D., Xia, F., & Jiang, N. (2009). Characterization of suspended

    solids in produced water in Daqing oilfield. Colloids and Surfaces A: Physicochemical and

    Engineering Aspects, 332(1), 63-69.

Di Pierro, S., Gnos, E., Grobety, B. H., Armbruster, T., Bernasconi, S. M., & Ulmer, P. (2003). Rock-forming moissanite (natural α-silicon carbide).American Mineralogist, 88(11-12), 1817-1821.

Doman L. (2015). U.S. remained world's largest producer of petroleum and natural gas hydrocarbons in 2014. (Available online: http://www.eia.gov/todayinenergy/detail.cfm?id=20692).

EIA. (2015a). U.S Field production of crude oil. (Available online: http://www.eia.gov/dnav/pet/hist/LeafHandler.ashx?n=PET&s=MCRFPUS2&f=A) (Accessed 04/30/2015)

EIA. (2015b). U.S. dry natural gas production. (Available online: http://www.eia.gov/dnav/ng/hist/n9070us2A.htm) (Accessed 04/30/2015)

EIA. (2015c). United States shale gas maps (available online: http://www.eia.gov/oil_gas/rpd/shale_gas.pdf) (accessed 4/30/2015)

Ellsworth, W. L. (2013). Injection-induced earthquakes. Science, 341(6142), 1225942.

Fakhru'l-Razi, A., Pendashteh, A., Abdullah, L. C., Biak, D. R. A., Madaeni, S. S., & Abidin, Z. Z. (2009). Review of technologies for oil and gas produced water treatment. Journal of Hazardous Materials, 170(2), 530-551.

Fehler, M., House, L., & Kaieda, H. (1987). Determining planes along which earthquakes occur: method and application to earthquakes accompanying hydraulic fracturing. Journal of Geophysical Research: Solid Earth (1978–2012), 92(B9), 9407-9414.

Gonzalez-Elipe, A. R., Espinos, J. P., Munuera, G., Sanz, J., & Serratosa, J. M. (1988). Bonding-state characterization of constituent elements in phyllosilicate minerals by XPS and NMR. The Journal of Physical Chemistry, 92(12), 3471-3476.

Goodwin, S., Carlson, K., Bai, B., Rein, L., Knox, K., & Douglas, C. (2013). Improved Water Use Estimates for Drilling and Hydrualic Fracturing in Northeastern Colorado. Journal of Water Resource and Protection, 5(12), 1262.

Guerra, K., Dahm, K., & Dundorf, S. (2011). Oil and gas produced water management and beneficial use in the Western United States. US Department of the Interior, Bureau of Reclamation.

Haasch, R. T. (2014). X-Ray Photoelectron Spectroscopy (XPS) and Auger Electron Spectroscopy (AES). In Practical Materials Characterization (pp. 93-132). Springer New York.

Huang, F., Gundewar, R., Steed, D., & Loughridge, B. (2006). Feasibility of using produced water for crosslinked gel-based hydraulic fracturing. VDI BERICHTE, 1940, 159.

Igunnu, E. T., & Chen, G. Z. (2012). Produced water treatment technologies. International Journal of Low-Carbon Technologies, cts049.

IHS Global Insight. (2011). The economic and employment contributions of shale gas in the United States.Prepared for America's Natural Gas Alliance by IHS Global Insight (USA), Washington, DC: America's Natural Gas Alliance.

Kimball, R. (2011). Key considerations for frac flowback/produced water reuse and treatment. In NJWEA Annual Conference (pp. 9-13).

King, G. E. (2012). Hydraulic fracturing 101: what every representative, environmentalist, regulator, reporter, investor, university researcher, neighbor and engineer should know about estimating frac risk and improving frac performance in unconventional gas and oil wells. In SPE Hydraulic Fracturing Technology Conference. Society of Petroleum Engineers.

King, R. F., & Morehouse, D. (1993). Drilling sideways—a review of horizontal well technology and its domestic application. US Department of Energy-Energy Information Administration April, 26.

Lechtenböhmer, S., Altmann, M., Capito, S., Matra, Z., Weindrorf, W., & Zittel, W. (2011). Impacts of shale gas and shale oil extraction on the environment and on human health. Wuppertal Institute for Climate, Environment and Energy and Ludwig-Bölkow-Systemtechnik GmbH, study requested by the European Parliament's Committee on Environment, Public Health and Food Safety, IP/A/ENVI/ST/2011-07, June.

Levine, A. D., Tchobanoglous, G., & Asano, T. (1991). Size distributions of particulate contaminants in wastewater and their impact on treatability. Water Research, 25(8), 911-922.

Malvern Instruments. (2012). Dynamic light scattering: an introduction in 30 minutes. Technical Note Malvern, MRK656-01, 1-8.

Odoma, A. N., Obaje, N. G., Omada, J. I., Idakwo, S. O., & Erbacher, J. (2015). Mineralogical, chemical composition and distribution of rare earth elements in clay-rich sediments from Southeastern Nigeria. Journal of African Earth Sciences, 102, 50-60.

Parrill, T. M., & Chung, Y. W. (1991). Surface analysis of cubic silicon carbide (001). Surface science, 243(1), 96-112.

Powers, K. W., Brown, S. C., Krishna, V. B., Wasdo, S. C., Moudgil, B. M., & Roberts, S. M. (2006). Research strategies for safety evaluation of nanomaterials. Part VI. Characterization of nanoscale particles for toxicological evaluation. Toxicological Sciences, 90(2), 296-303.

Riemer, P. (1996). Greenhouse gas mitigation technologies, an overview of the CO 2 capture,

    storage and future activities of the IEA greenhouse gas R&D programme. Energy

    Conversion and Management, 37(6), 665-670.

Sasaki, S. (1998). Characteristics of microseismic events induced during hydraulic fracturing

    experiments at the Hijiori hot dry rock geothermal energy site, Yamagata,

    Japan. Tectonophysics, 289(1), 171-188.

US Energy Information Administration (EIA) (2014). Annual Energy Outlook 2014. Report

    Number: DOE/EIA-0383(2014).

Vempati, R. K., Loeppert, R. H., Dufner, D. C., & Cocke, D. L. (1990). X-ray photoelectron

    spectroscopy as a tool to differentiate silicon-bonding state in amorphous iron oxides. Soil

    Science Society of America Journal, 54(3), 695-698.

Werne, J. P., Sageman, B. B., Lyons, T. W., & Hollander, D. J. (2002). An integrated assessment

    of a "type euxinic" deposit: evidence for multiple controls on black shale deposition in the

    Middle Devonian Oatka Creek Formation.American Journal of Science, 302(2), 110-143.

Ziemkiewicz, P., Quaranta, J. D., & McCawley, M. (2014). Practical measures for reducing the

    risk of environmental contamination in shale energy production. Environmental Science:

    Processes & Impacts, 16(7), 1692-1699.

Zielinski, R. A., & Otton, J. K. (1999). Naturally Occurring Radioactive Materials (NORM) in

    Produced Water and Oil-field Equipment: An Issue for Energy Industry. US Department of

    the Interior, US Geological Survey.

Appendix A Particle Size Distribution

Crow Creek Pad wells CC-73 and CC-76-1
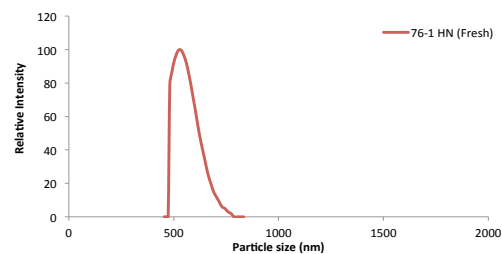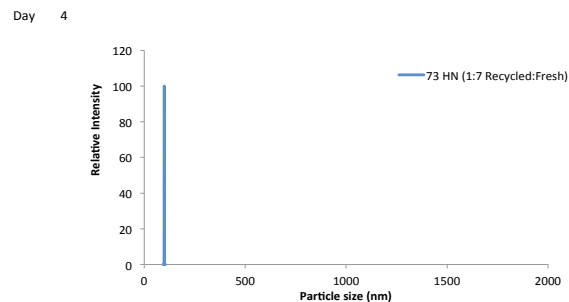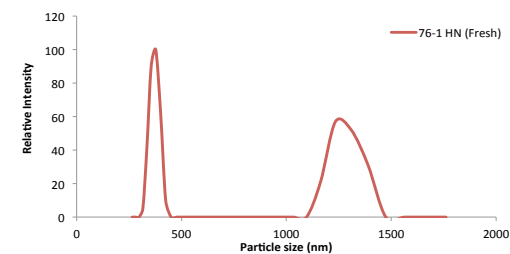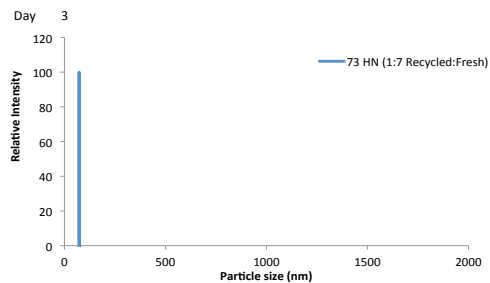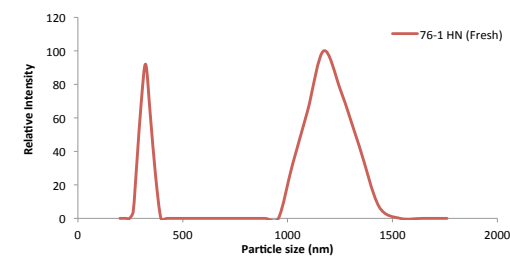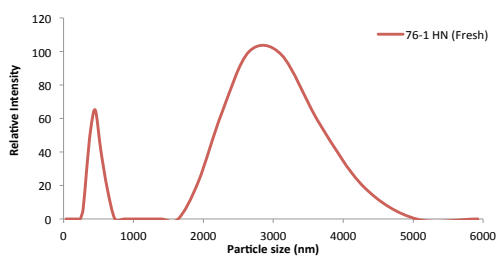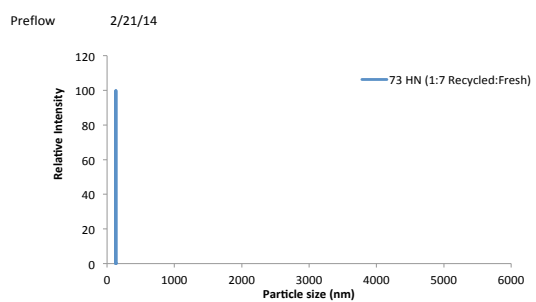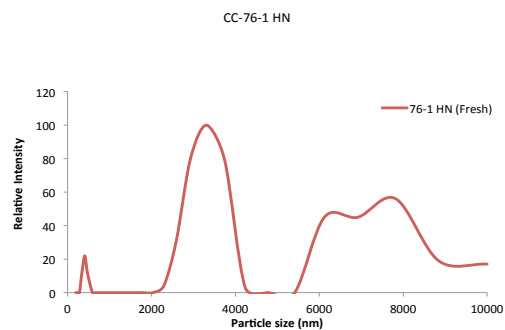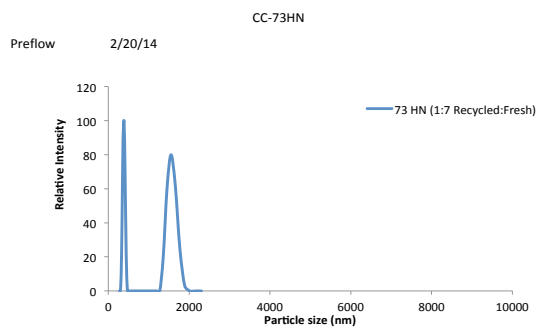
Day   5
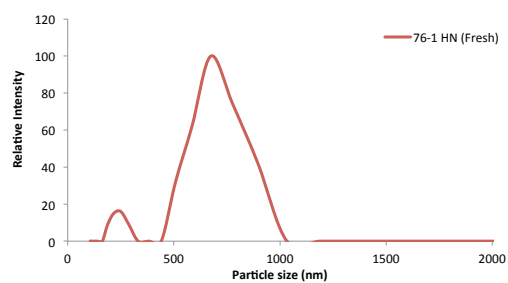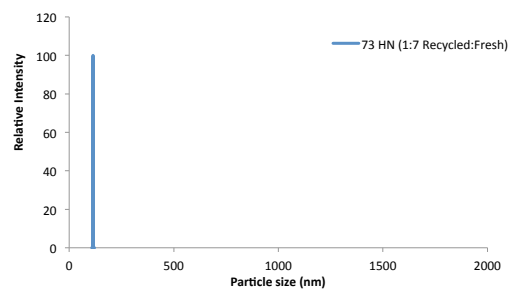
Day   6

Day   7

Day   8

Day   9

53
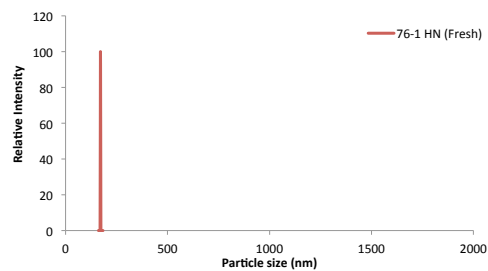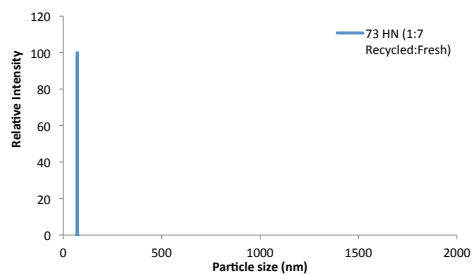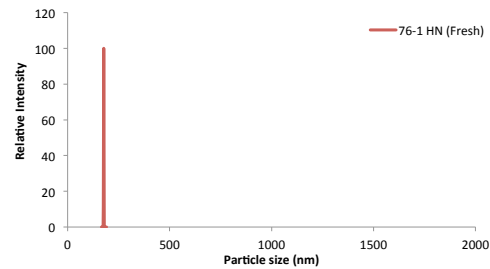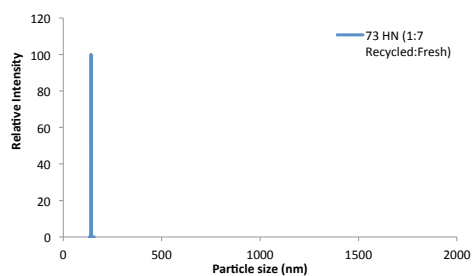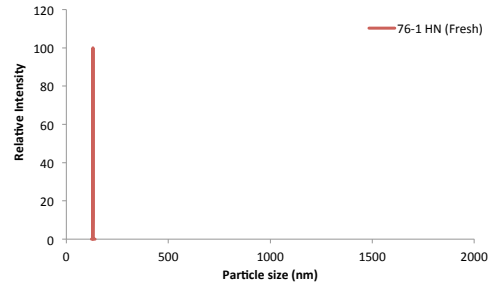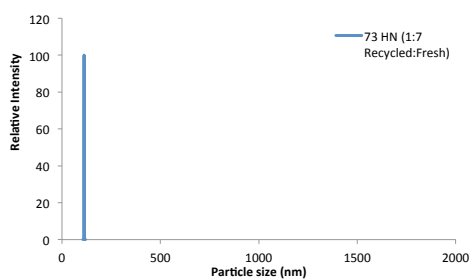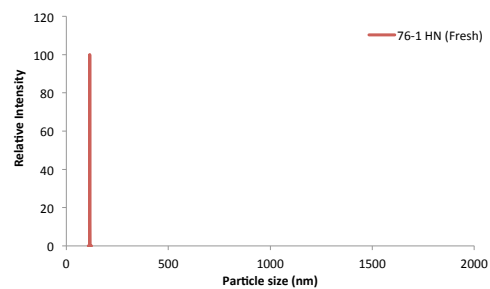
Day   11
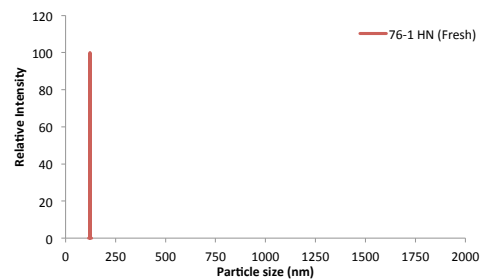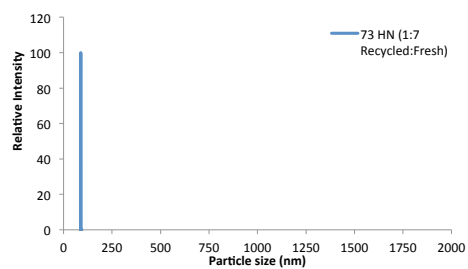
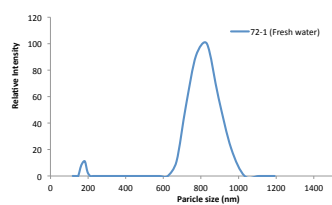Day   12
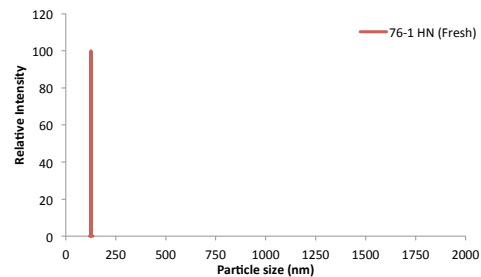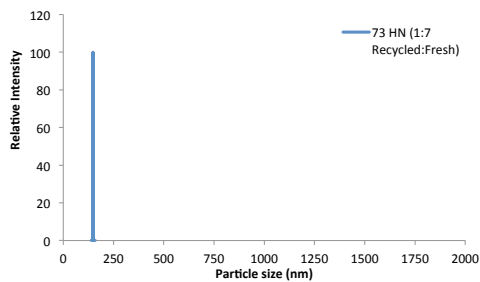
Day   13
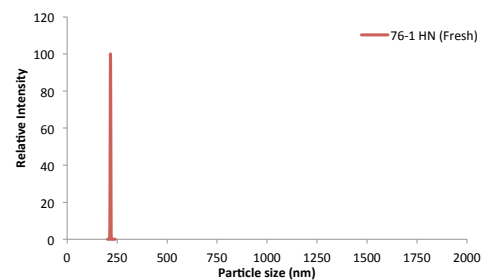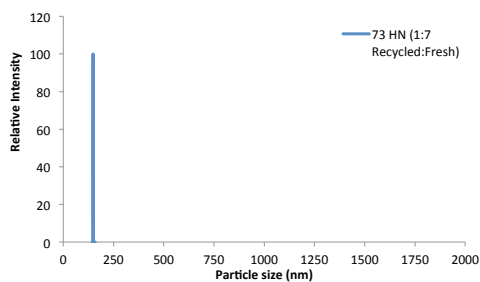
Day   14
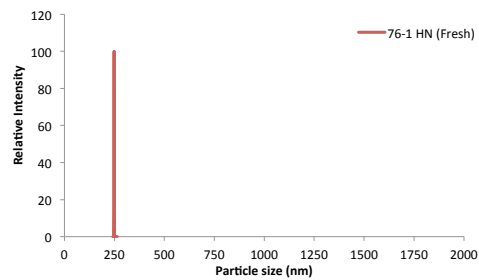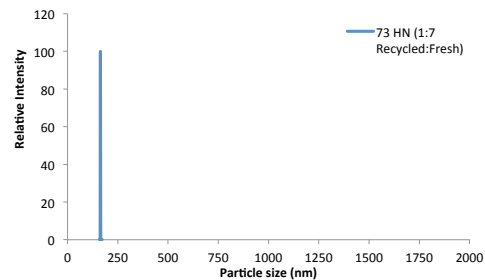
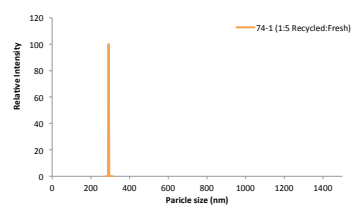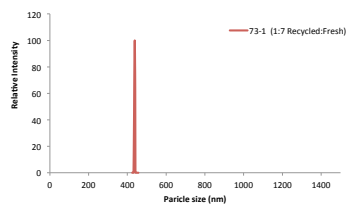
Day   15
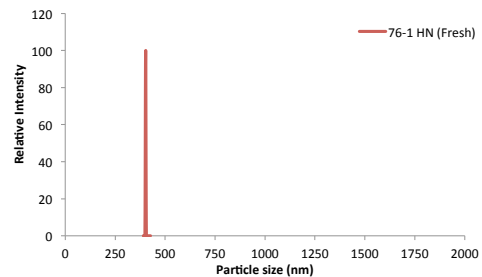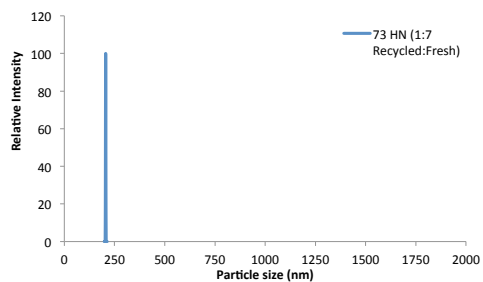
Day 18
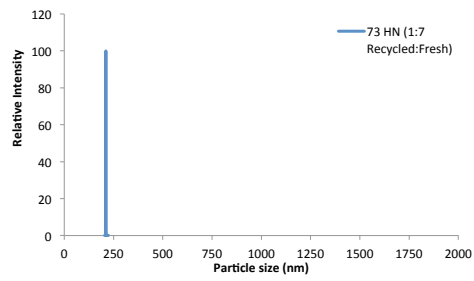
Day 21
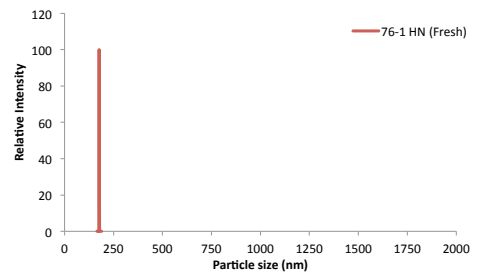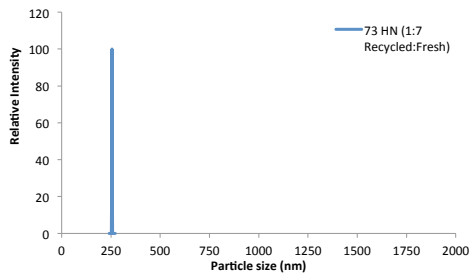
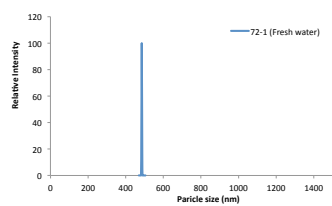Day 24
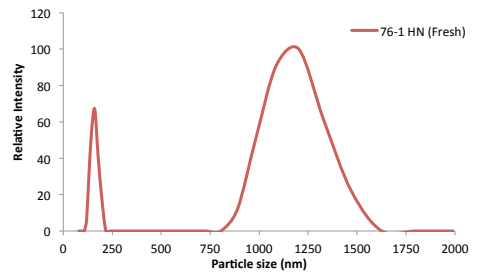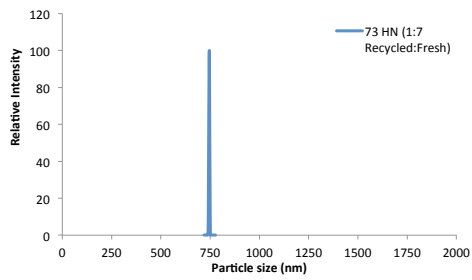
Day 30
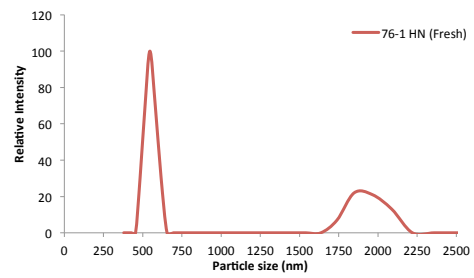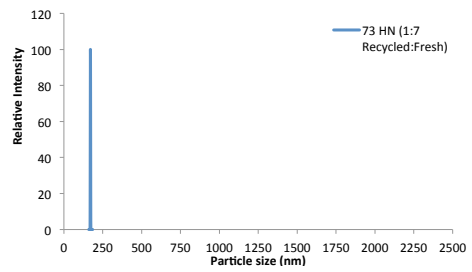
Chandler State wells 72-1, 73-1 and 74-1:
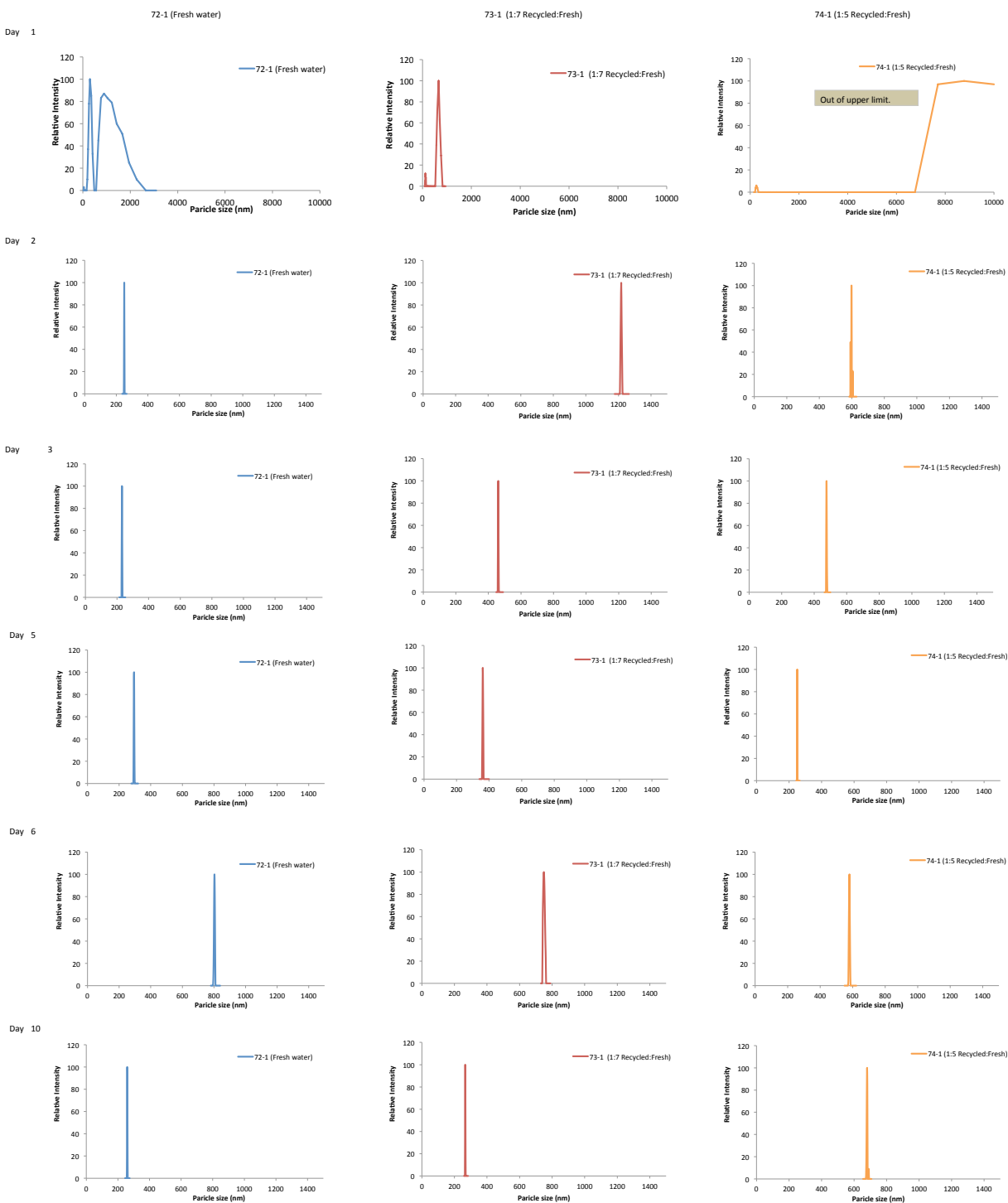
Day 14
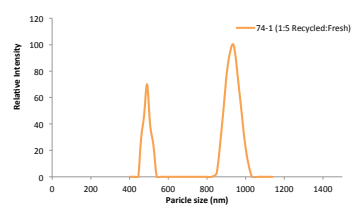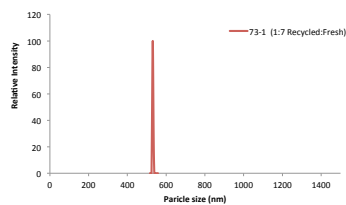
Day 20

Appendix B. XPS Survey Scan Spectra
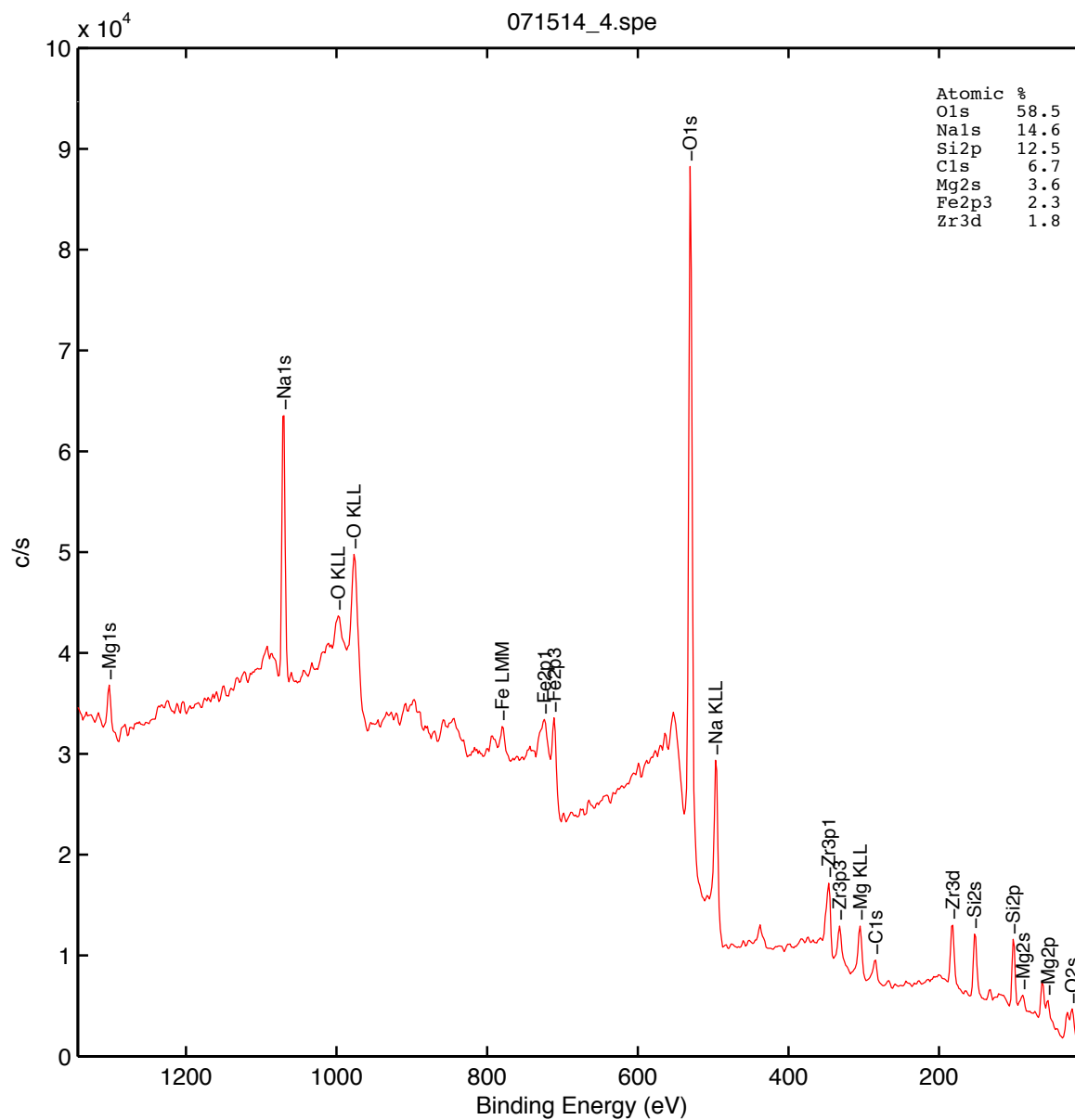
CS-72-1 Day 1

071514_1.spe: 72–Day1		Company Name
2014 Jul 15 Al mono 350.0 W 0.0 45.0° 187.85 eV	4.2737e+004 max	1.82 min
Sur1/Full/1 (Shft SG5)		

071514_1.spe

Atomic %
O1s	58.3
Na1s	12.8
Si2p	12.1
C1s	6.6
Ca2p	3.6
Fe2p3	2.5
Zr3d	1.7
Mg2s	1.5
Cl2p	1.0

CS-73-1 day 1

071514_4.spe

Atomic %
O1s   58.5
Na1s   14.6
Si2p   12.5
C1s   6.7
Mg2s   3.6
Fe2p3   2.3
Zr3d   1.8

CS-74-1 day 1

CS-72-1 day 2
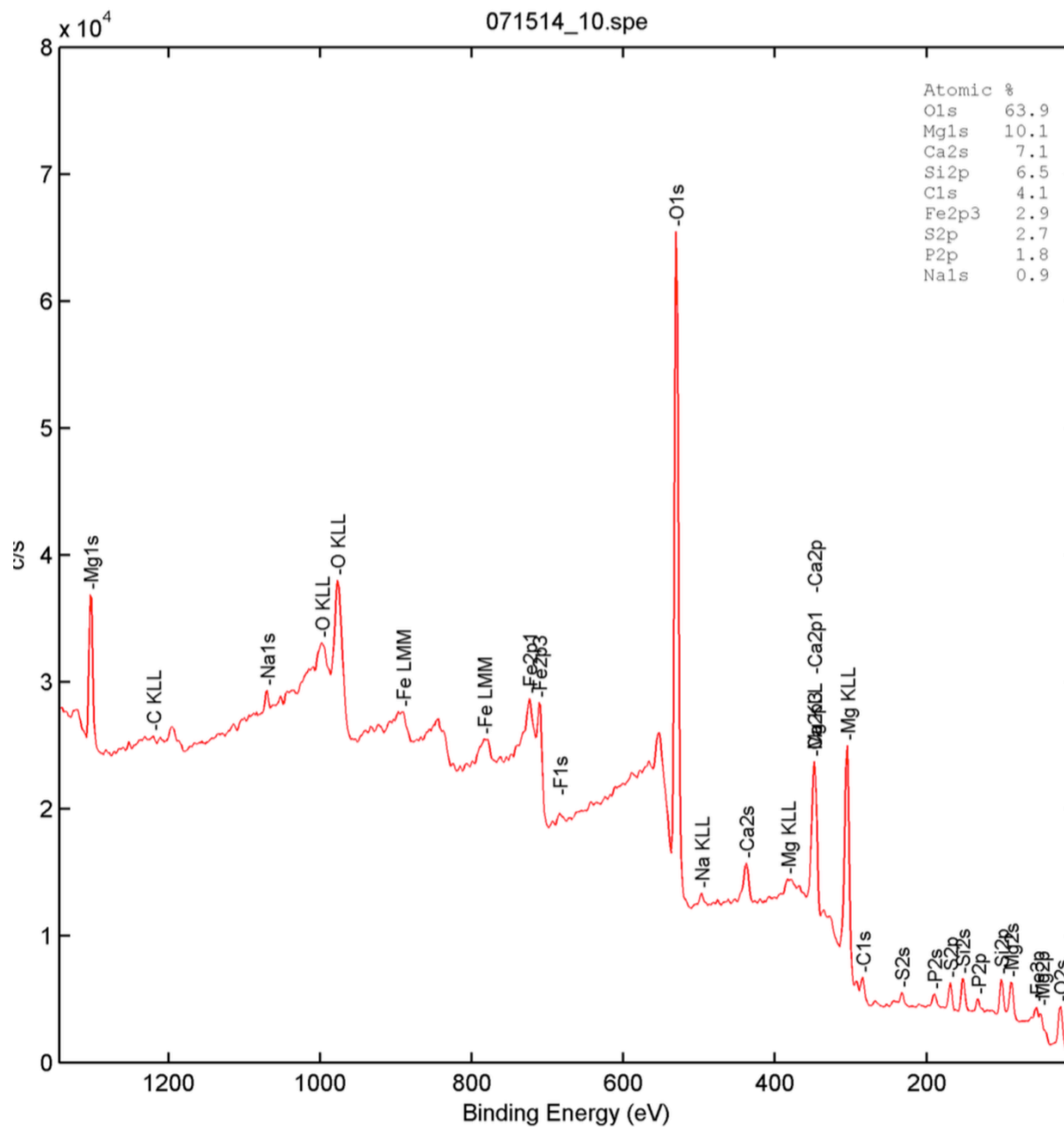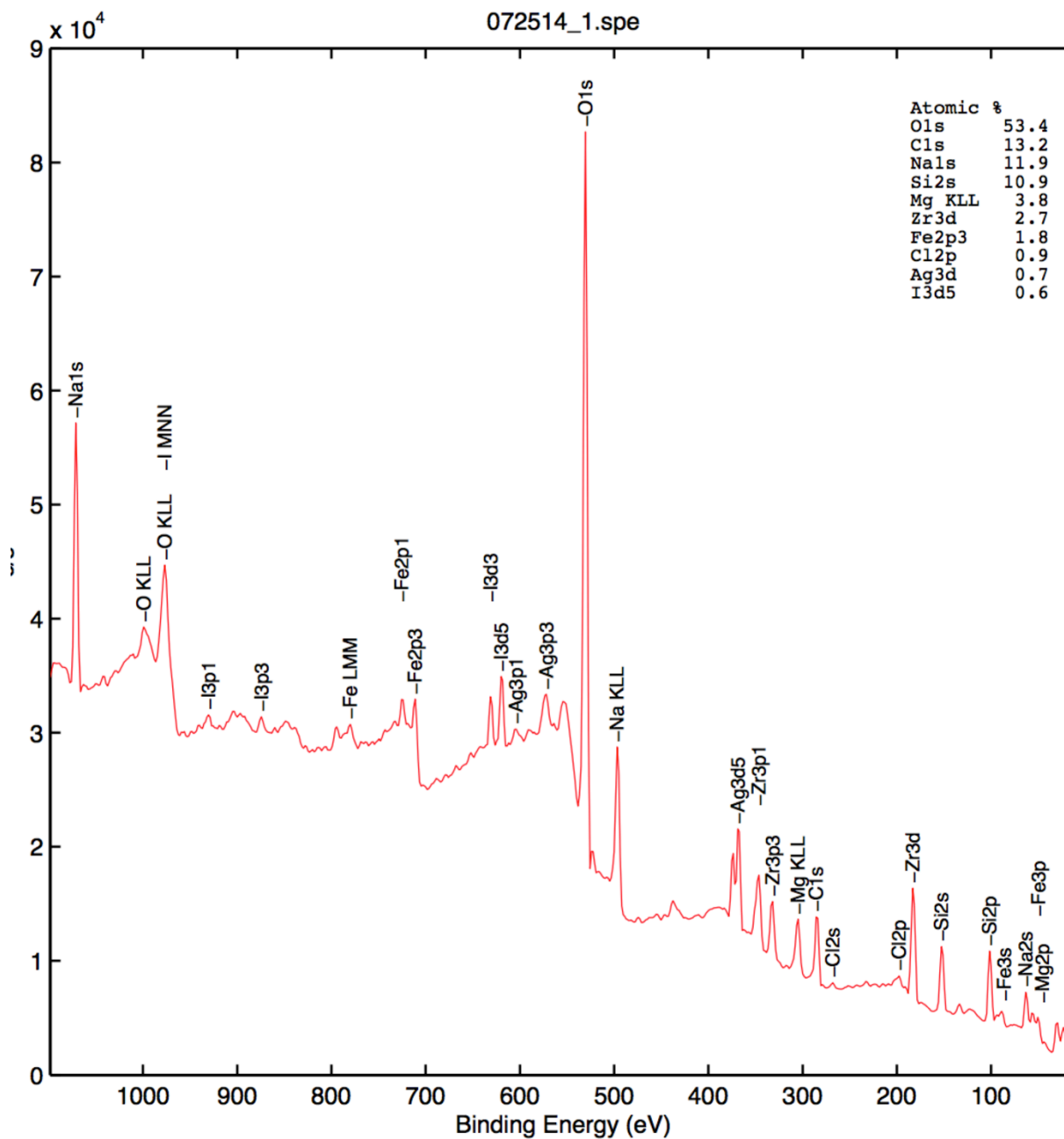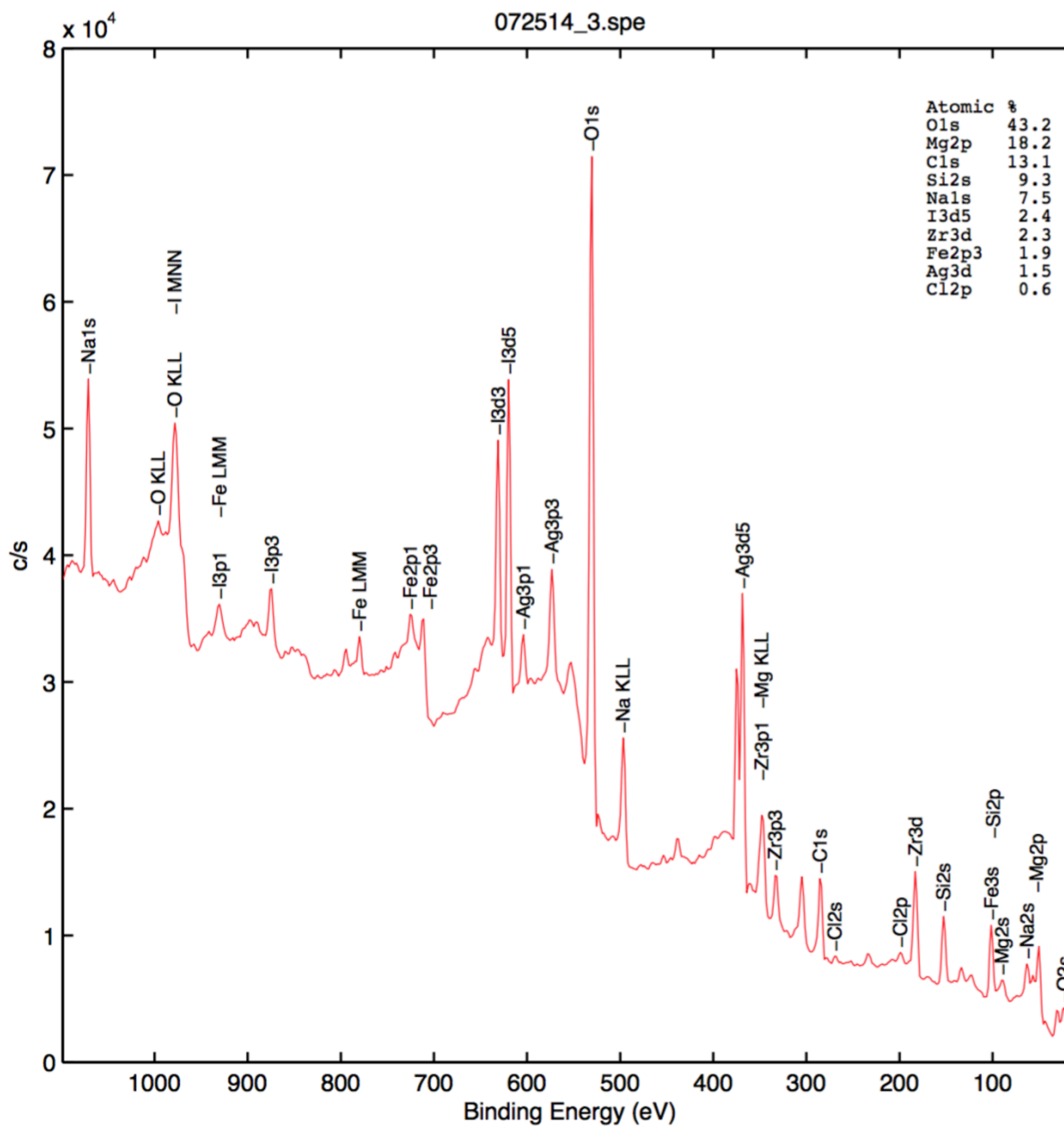

072514_1.spe: 72_day2   Company Name

2014 Jul 25 Al mono 350.0 W 0.0 45.0° 187.85 eV   8.2692e+004 max   4.77 min

Sur1/Full/1 (SG5 Shft Shft)

Atomic %	
O1s	53.4
C1s	13.2
Na1s	11.9
Si2s	10.9
Mg KLL	3.8
Zr3d	2.7
Fe2p3	1.8
Cl2p	0.9
Ag3d	0.7
I3d5	0.6

CS-73-1 day 2

072514_3.spe: 73_day2   Company Name

2014 Jul 25 Al mono 350.0 W 0.0 45.0° 187.85 eV   7.1449e+004 max   4.77 min
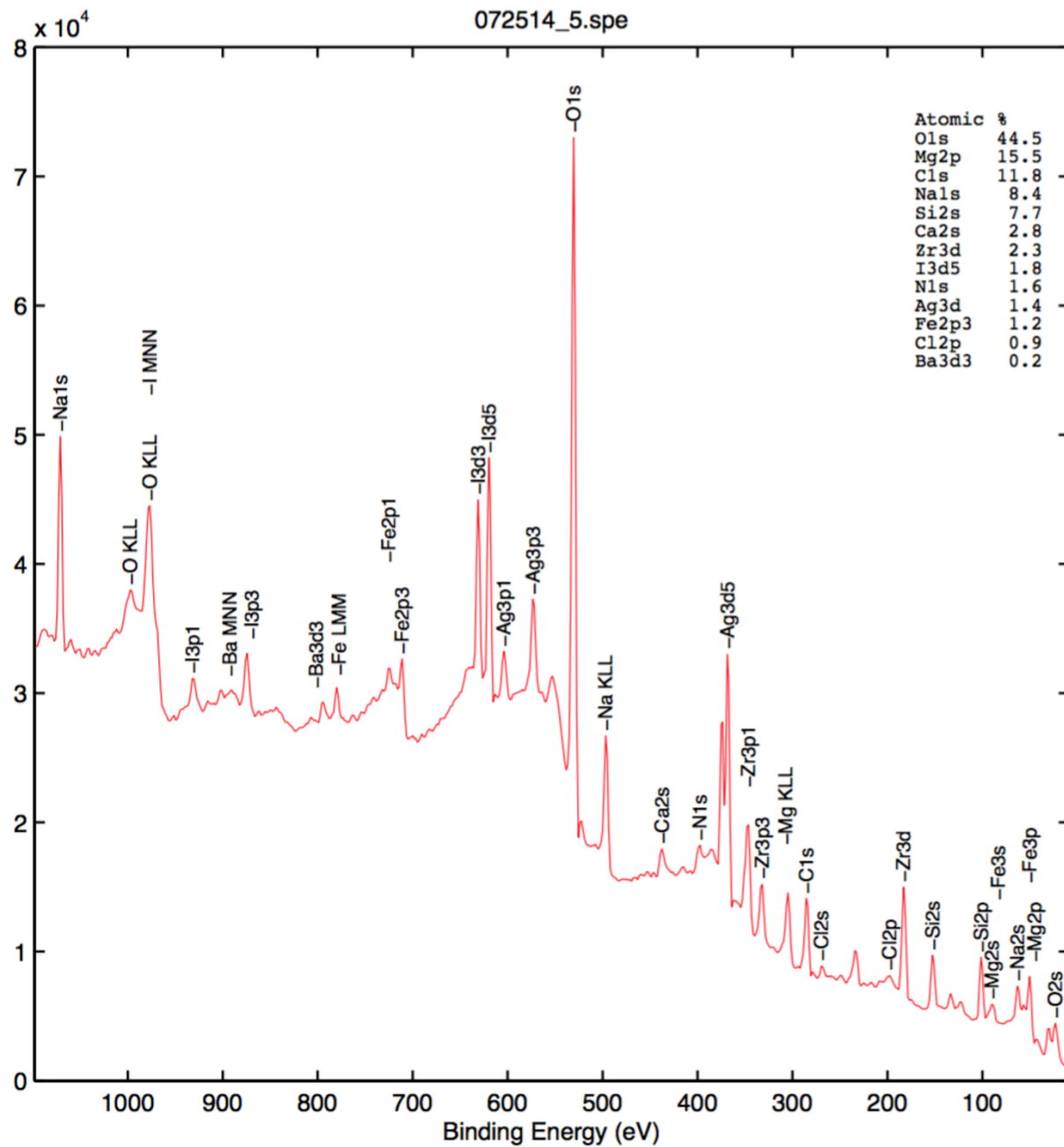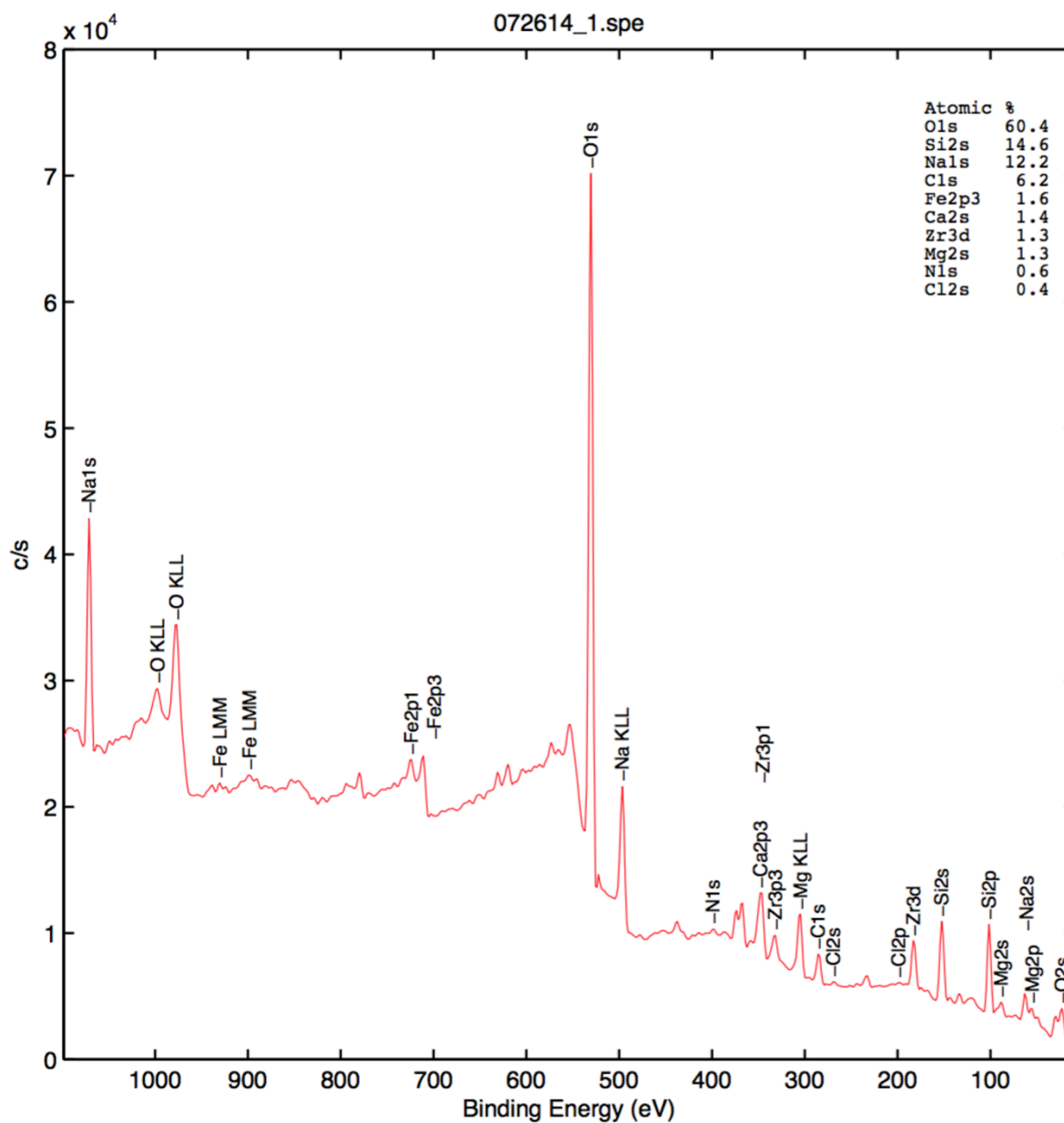
Sur1/Full/1 (SG5 Shft)

x 10⁴

072514_3.spe

c/s

Atomic %
O1s   43.2
Mg2p   18.2
C1s   13.1
Si2s   9.3
Na1s   7.5
I3d5   2.4
Zr3d   2.3
Fe2p3   1.9
Ag3d   1.5
Cl2p   0.6

–Na1s
–O KLL
–O KLL
–I MNN
–Fe LMM
–I3p1
–I3p3
–Fe LMM
–Fe2p1
–Fe2p3
–I3d3
–I3d5
–O1s
–Ag3p1
–Ag3p3
–Na KLL
–Ag3d5
–Zr3p1
–Mg KLL
–Zr3p3
–C1s
–Cl2s
–Cl2p
–Zr3d
–Si2s
–Mg2s
–Fe3s
–Na2s
–Si2p
–Mg2p
–O2s

Binding Energy (eV)

CS-74-1 day 2

CS-72-1 day 6

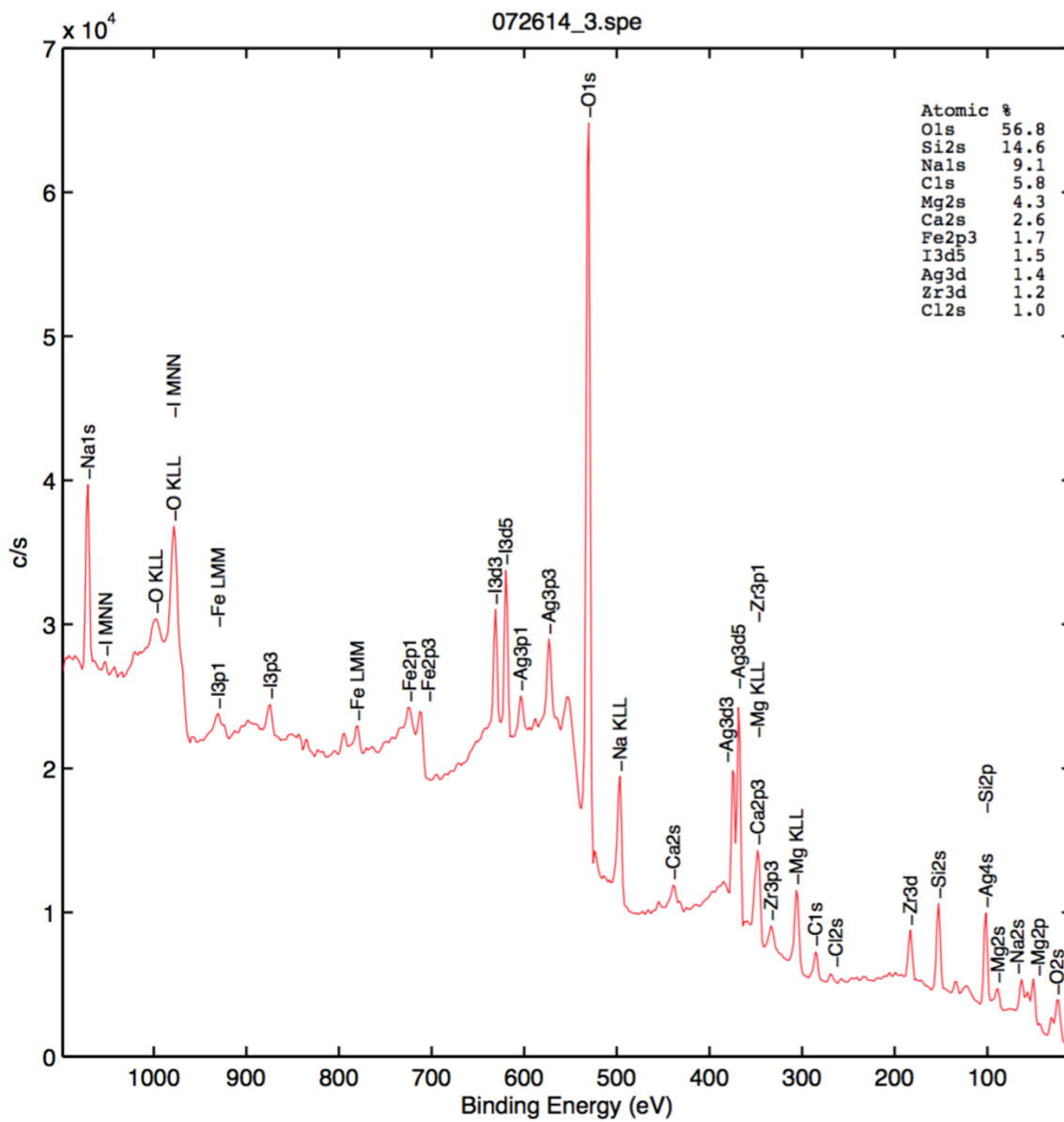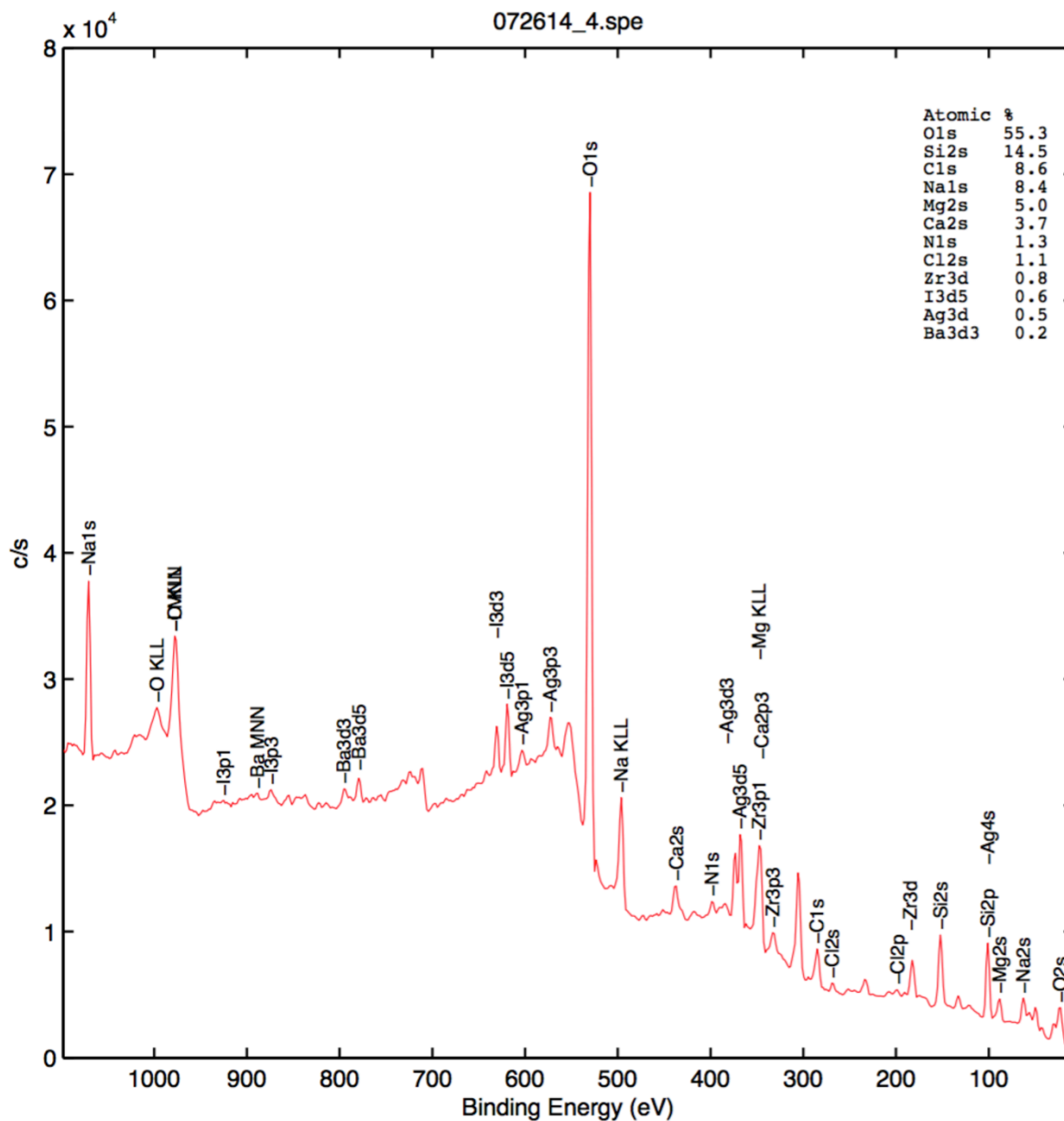CS-73-1 day 6

072614_3.spe: 73_DAY6   Company Name

2014 Jul 31 Al mono 350.0 W 0.0 45.0° 187.85 eV   6.4804e+004 max   4.77 min

Sur1/Full/1 (SG5 Shft)

072614_3.spe

Atomic %
O1s   56.8
Si2s   14.6
Na1s   9.1
C1s   5.8
Mg2s   4.3
Ca2s   2.6
Fe2p3   1.7
I3d5   1.5
Ag3d   1.4
Zr3d   1.2
Cl2s   1.0
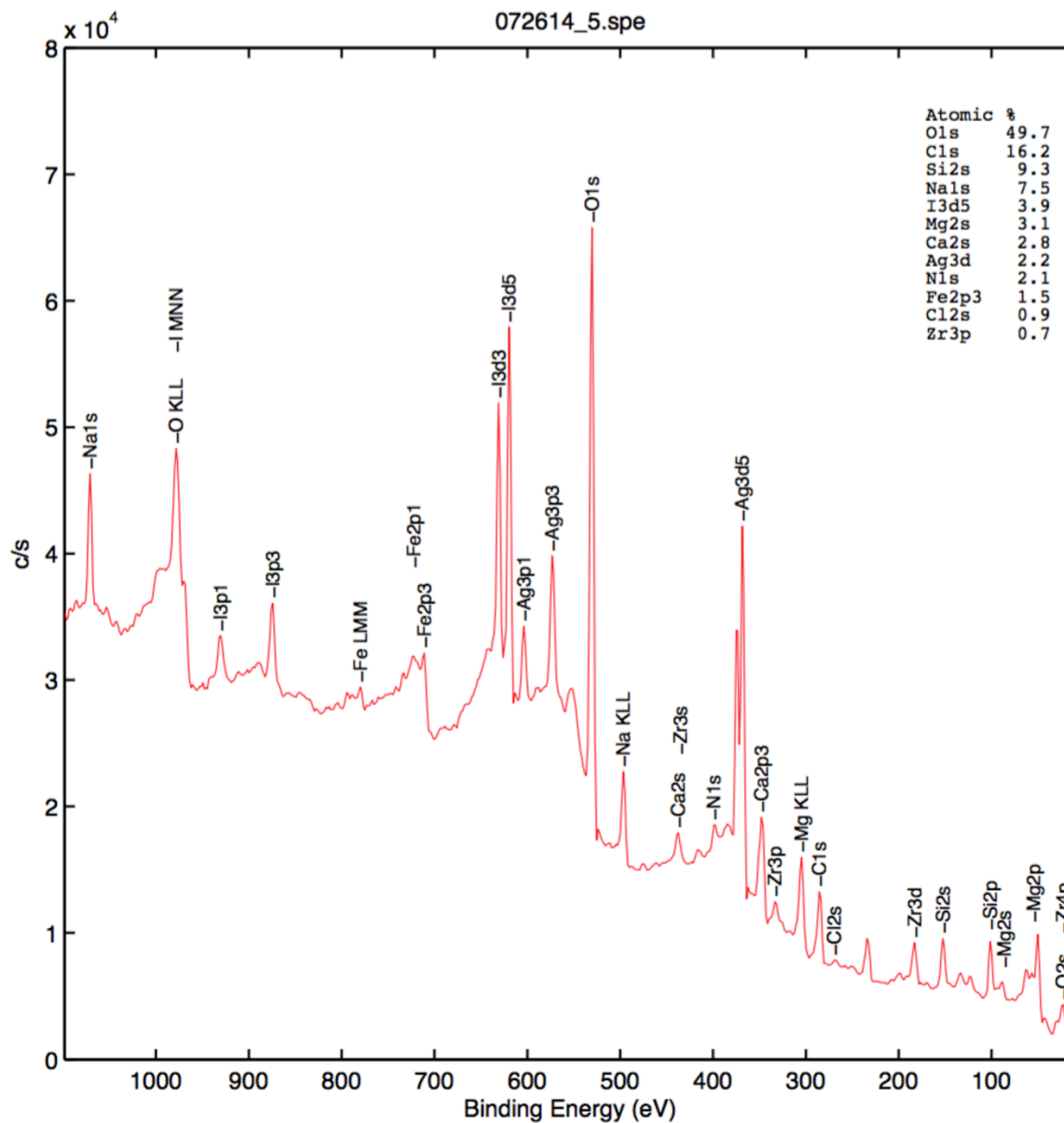
CS-74-1 day 6

072614_4.spe: 74_DAY6   Company Name

2014 Jul 31 Al mono 350.0 W 0.0 45.0° 187.85 eV   6.8554e+004 max   3.86 min

Sur1/Full/1 (SG5 Shft)

072614_4.spe

x 10⁴

Atomic %	
O1s	55.3
Si2s	14.5
C1s	8.6
Na1s	8.4
Mg2s	5.0
Ca2s	3.7
N1s	1.3
Cl2s	1.1
Zr3d	0.8
I3d5	0.6
Ag3d	0.5
Ba3d3	0.2

c/s

Binding Energy (eV)

CS-72-1 day 10

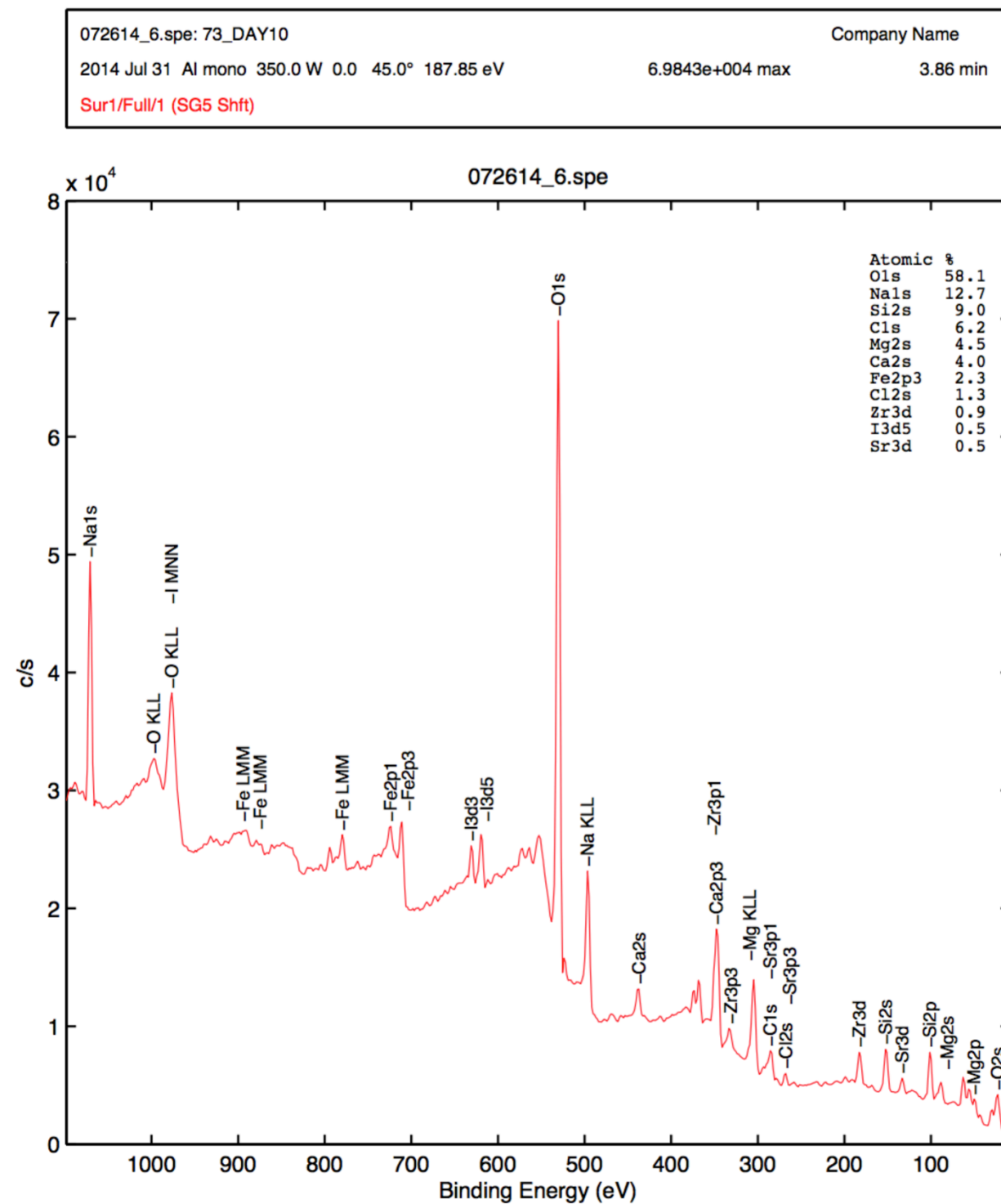072614_5.spe: 72–DAY10   Company Name

2014 Jul 31 Al mono 350.0 W 0.0 45.0° 187.85 eV   6.5764e+004 max   3.86 min
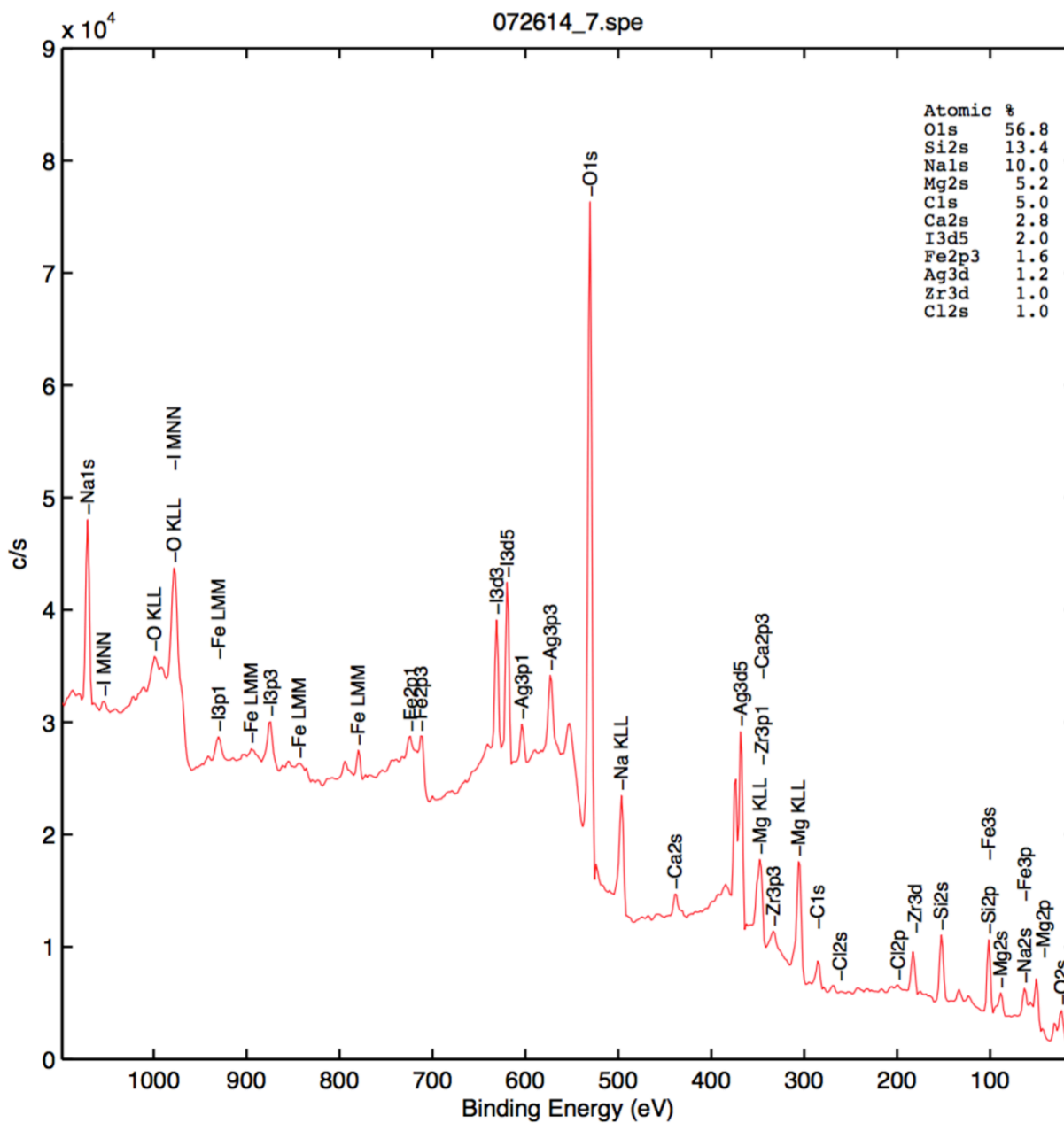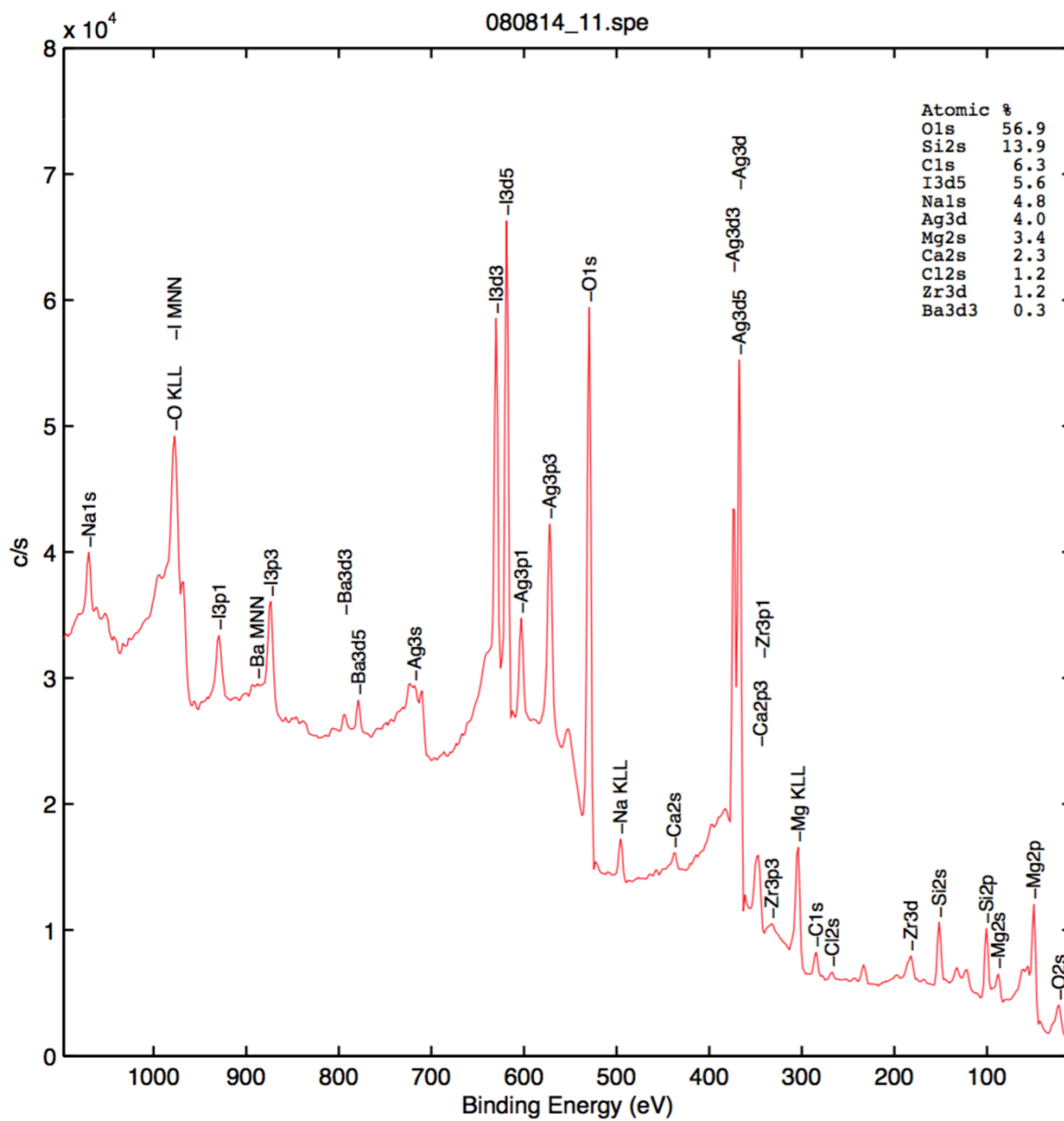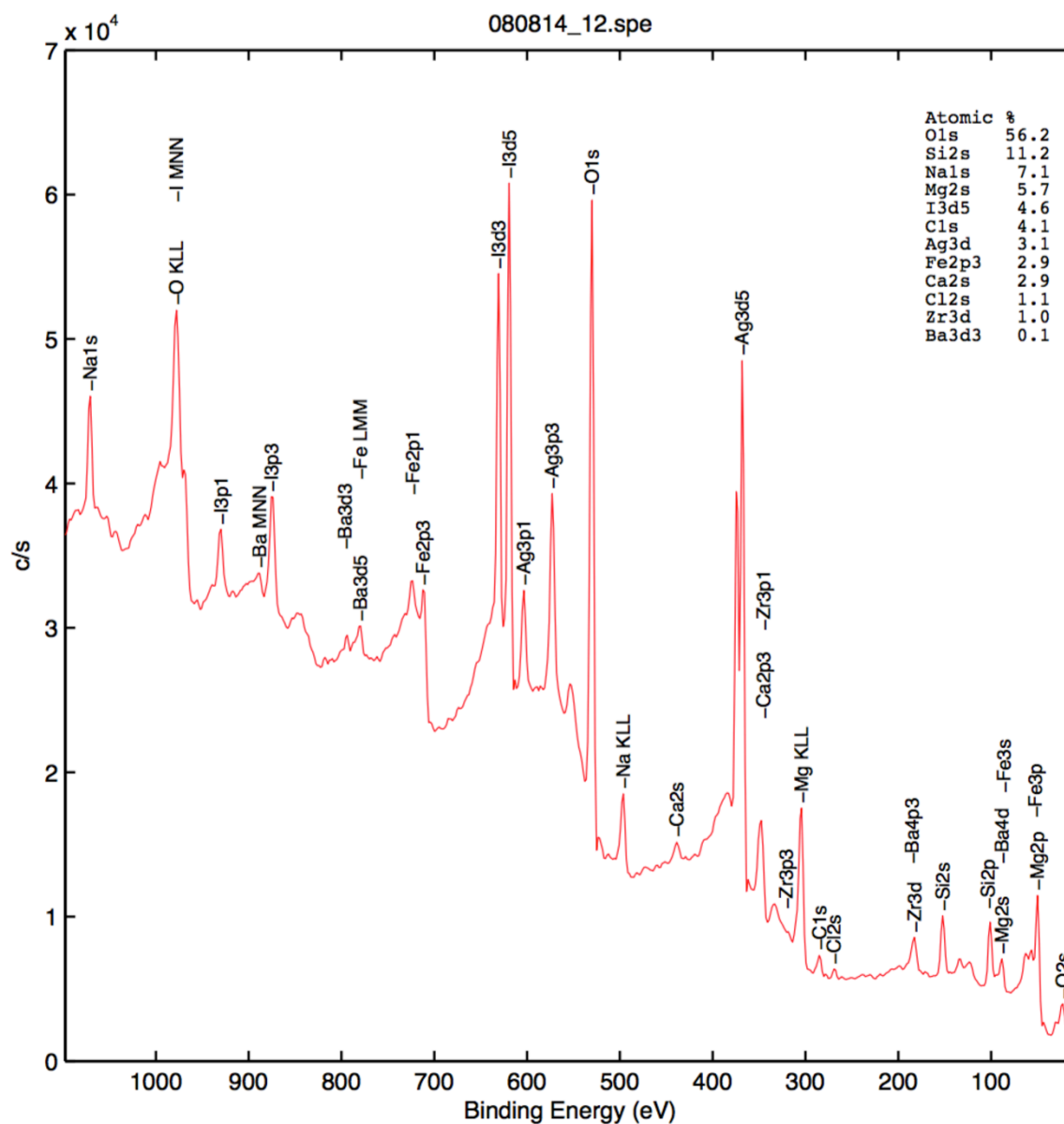
Sur1/Full/1 (SG5 Shft)

072614_5.spe

x 10⁴

Atomic %
O1s   49.7
C1s   16.2
Si2s   9.3
Na1s   7.5
I3d5   3.9
Mg2s   3.1
Ca2s   2.8
Ag3d   2.2
N1s   2.1
Fe2p3 1.5
Cl2s   0.9
Zr3p   0.7

CS-73-1 day 10

CS-74-1 day 10

072614_7.spe

x 10^4

c/s

Binding Energy (eV)

Atomic	%
O1s	56.8
Si2s	13.4
Na1s	10.0
Mg2s	5.2
C1s	5.0
Ca2s	2.8
I3d5	2.0
Fe2p3	1.6
Ag3d	1.2
Zr3d	1.0
Cl2s	1.0

Peak labels: Na1s, I MNN, O KLL, I MNN, Fe LMM, I3p1, Fe LMM, I3p3, Fe LMM, Fe LMM, Fe2p1, Fe2p3, I3d3, I3d5, Ag3p1, Ag3p3, O1s, Na KLL, Ca2s, Ag3d5, Zr3p1, Ca2p3, Mg KLL, Zr3p3, Mg KLL, C1s, Cl2s, Cl2p, Zr3d, Si2s, Fe3s, Si2p, Mg2s, Na2s, Fe3p, Mg2p, O2s

CS-72-1 day 20

CS-73-1 day 20

CS-74-1 day 20